

Extending USArray into Canada -- Pascal Audet, UC Berkely

Earthscope, in particular the USArray Transportable and Flexible Array components, has enabled the construction of high-resolution, three-dimensional models of the continental crust and mantle at scales ranging from continental (e.g., western US upper mantle) to regional (e.g., subducting oceanic crust in the Cascadia forearc, lithospheric mantle drips in California) in the lower 48. The success of Earthscope in the western US bears a lot of promise for the study of active processes in Alaska, in particular in terms of plate collision, mountain building, strike-slip faulting, subduction, and volcanism. Unfortunately, the lack of coverage in western Canada between Alaska and the Pacific Northwest, where these systems may be kinematically linked, impedes a comprehensive investigation of western North American tectonics. The extension of USArray into Canada is a unique opportunity to rectify this situation by leveraging resources and reducing technical difficulties associated with deployment in a challenging environment. In this paper I outline a few key scientific questions that will benefit from a joint Canada-US effort to extend the USArray TA into northwestern Canada.

Yakutat collision and subduction

Shallow subduction of the Yakutat Block beneath the North America continent is believed to be responsible for the continuing uplift of the Chugach-Saint Elias Mountains. The subduction of the Yakutat Block has been studied in its western extension beneath Alaska from the BEAAR Array (Eberhart-Phillips et al., 2006). However, its northeastern and eastern extension remains unknown due to a lack of seismic instrumentation on the Canadian side. Key questions to investigate include the geometry and velocity structure of the downgoing plate, their relation to slab seismicity and metamorphic evolution, the pattern of mantle flow and fabric associated with slab edge subduction, etc.

Northern Cordillera and Arctic

The Yakutat collision is thought to provide enough force to drive deformation as far inland as the Cordillera-Craton transition at the Deformation Front (~1000 km away), and possibly to the north within the Arctic Basin (Mazzotti et al., 2008). Understanding the stress transfer across such long distances requires knowledge of crustal structure (geometry and composition), the depth extent of seismogenic faults, and lithospheric temperatures that can be obtained with regional seismic networks such as the TA deployment.

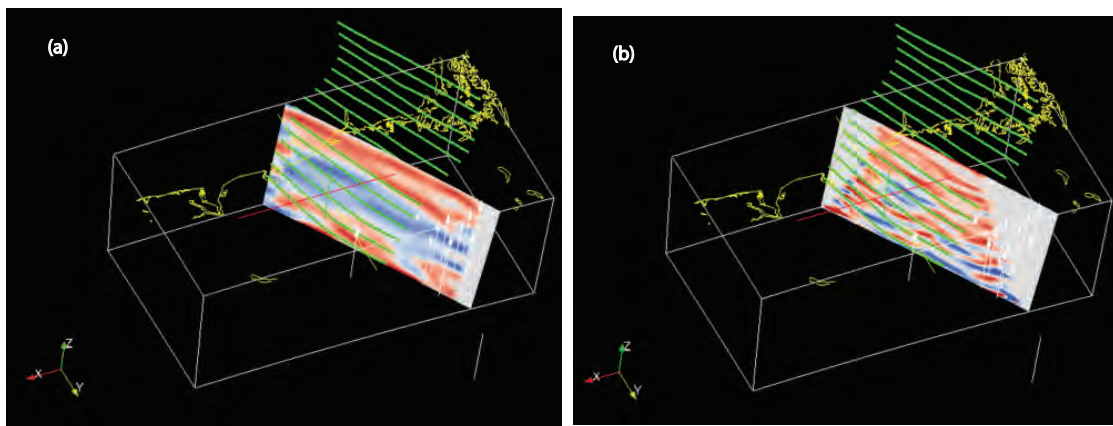
Coast Plutonic Complex

The Coast Plutonic Complex (CPC) is the largest batholith on Earth, and is presumably underlain by an ultramafic root. In light of results of lithospheric foundering of the root beneath the Sierra Nevada (Zandt et al., 2004), it is reasonable to assume that such process has operated in the past beneath the CPC. Providing seismic images of the deep structure of the COC from northern Cascadia to southeastern Alaska will undoubtedly improve our knowledge on the evolution and lithospheric delamination of magmatic arc systems, and on the long-term evolution of crustal composition in general.

Converted Wave Imaging of the Subducting Yakatat Lithosphere

Mark Bauer and Gary L. Pavlis, Department of Geological Sciences, Indiana University, 1001 East 10th, Bloomington, IN 47405 (mbauer@indiana.edu, pavlis@indiana.edu)

We have analyzed broadband seismic data from the STEEP project using P and S receiver functions shown in this figure. S data were processed using conventional Common Conversion Point (CCP) stacking while the P data were processed with CCP stacking and a recently developed three-dimensional, plane-wave migration technique. The S data (a) show a clearer but lower resolution image of the subducting Yakatat lithosphere. Sediment reverberations observed for stations on the Yakatat block are a problem with the P data (b). The results shown in this figure reduced the impact of this problem in a novel way by not mixing data from Yakatat block stations with stations to the north and east. Both data sets illuminate a gently dipping, positive conversion horizon we interpret as the top of the subducting Yakatat lithosphere. We find the dip of this feature to increase consistently from around 18° in Prince William Sound to around 20° near Icy Bay. A strong, secondary argument that this feature is the top of the subducting plate is that the down dip projection of this horizon to the map locations of the Wrangell volcanoes is entirely consistent with global averages for the depth to the top of the slab measured in other subduction zones. The flow lines in the slab model illustrated also indicate that the eastern edge of the Wrangells project directly to the area of very rapid uplift revealed by STEEP on the eastern side of Mt St Elias. This is additional evidence that Mt St Elias is the nexus of deformation in this tectonic corner. The actual eastern edge of the Pacific plate is, however, poorly imaged by the STEEP data because of a lack of coverage east of Mt St Elias. Resolving the geometry in this tectonic corner will be an important target for Earthscope.



Receiver function imaging results from STEEP. (a) shows a section through S receiver function image volume and (b) is the same section through the P image volume. Coastline is shown in this 3D perspective as a yellow curve. The green lines illustrate a model for the top of the slab. The model was produced from joint interpretations of these image volumes with the updip side constrained by the location of the trench. The lines are flow lines computed for Pacific-North America motion drawn along the top of the Yakatat lithosphere defined by this model. The white lines extend from the surface position of the Wrangell volcanoes to a depth of 100 km.

Geophysical Investigations into the Tectonic and Magmatic Evolution of Southwest Alaska

Paul A Bedrosian, Eric D. Anderson, Anjana K. Shah, and Karen D. Kelley

US Geological Survey, Crustal Geophysics & Geochemistry Science Center, Denver, CO

Large swaths of Alaska are concealed by glacial or volcanic cover. These regions represent one of the largest uncertainties in national and global mineral resource assessments, as carried out by the US Geological Survey's Mineral Resources Program. As part of an effort to improve these assessments, the USGS is carrying out a range of geophysical investigations in Southern Alaska (Fig. 1). These investigations have focused on understanding the tectonic and magmatic evolution of the region in addition to more targeted studies of known regions of mineralization.

The Jura-Cretaceous Kahiltna Terrane, situated between the Peninsular Terrane to the south and the Kuskokwim Group sedimentary package to the north, is not well-defined in terms of its boundaries, its internal structure, or its extensive magmatic history. The geometry of the Mulchatna fault zone, generally believed to be the northern boundary of the Kahiltna Terrane, becomes increasingly speculative to the west, as do structures such as the Lake Clark Fault, interpreted by some as the southern Kahiltna Terrane boundary. Though mostly concealed beneath glacial and volcanic cover, K/Ar and Ar/Ar dating of rocks within the Kahiltna Terrane and beyond indicates at least three magmatic pulses (90Ma, 65Ma, 45Ma).

The USGS collected magnetotelluric and gravity data over a 10,000 km² area within the central and northern Kahiltna Terrane (Fig. 2). Regional aeromagnetic data provide the broader context for these studies. When examined in concert with age dates and catalogs of known mineralization, a reconstruction of the mainly buried, subduction-related Late Cretaceous paleo-magmatic arc can be attempted. Both magnetic data and a 3D resistivity model reveal a first-order change in crustal structure across a sinuous thrust boundary south of the Mulchatna Lineament. This boundary is paralleled by a series of linear magnetic highs and lows which we interpret as upturned sediments or metasediments associated with compression during or after suturing of the Kahiltna to the Kuskokwim. Within the central Kahiltna Terrane, large intrusives make up a significant crustal volume, with resistivity models constraining the geometry and extent of the intrusions from mid-crustal depths to at or near the surface. Gravity data can then be used to differentiate between felsic and mafic intrusives as well as overlying volcanic rocks

A particularly large intrusive cluster, parts of which date to 90Ma, is delineated by both magnetics and magnetotellurics. This cluster is associated with the world-class Pebble Cu-Au-Mo porphyry deposit and a number of associated skarns and base-metal deposits. A strong conductive zone is imaged at mid-crustal depths beneath this cluster, and may be associated with large-scale processes that led to the shallow mineralization. Alternatively, the high conductivity may reflect a zone of crustal weakness along the Lake Clark Fault corridor, which intersects this large intrusive cluster.

In much the same way that Earthscope Flexible Array studies within the continental US have built upon the Transportable Array, regional studies in Alaska will benefit greatly from having Transportable Array coverage of Alaska. As the studies above illustrate, one of the greatest challenges in developing mineral resource assessments in Alaska is in understanding the tectonic framework at scales ranging from mineral districts to terranes to the entire state. In Alaska, individual surveys with limited aperture often suffer from a lack of context; bringing the Earthscope Transportable Array to Alaska would provide much needed 'infrastructure' and allow existing and new surveys to be interpreted in a new light.

Informing Earthquake Geology Through Seismology – and the Other Way Around

Sean P. Bemis – U.S. Geological Survey and University of Kentucky

Studies over the past 10 years have rapidly expanded our recognition of Quaternary-active faults in south-central Alaska. Additionally, many of these faults are recognized as active during the Holocene, and thus represent potential seismogenic sources. However, many of the major active crustal faults in Alaska with clear evidence of recurrent Holocene earthquakes have been seismically quiet during historic times. Although this is expected given the duration of a typical seismic cycle relative to the short historical record, we also recognize prominent zones of crustal seismicity (outside of aftershock sequences) that display no evidence for recent earthquake surface rupture.

Possible explanations for this apparent difference in fault behavior include:

- 1) Earthquake geologists have not invested in detailed mapping efforts along the active seismicity lineaments/zones, and thus surface-rupturing earthquakes have occurred but remain unrecognized.
- 2) The seismicity lineaments/zones relieve most of their strain accumulation in small earthquakes, and thus do not produce significant surface-rupturing earthquakes
- 3) The faults that do produce large surface-rupturing earthquakes do have background seismicity, but much of it is below the detection limit of the current seismic network.
- 4) Fundamental physical properties differ between each type of fault zone, possibly related to the involved lithologies, the cumulative displacement (fault zone development), etc.
- 5) Patterns of background seismicity change through the course of a seismic cycle.

These are certainly not the only likely explanations, but they do include aspects that we know to be true, and other aspects that will be testable with EarthScope data. Addressing these issues will contribute to our understanding of fundamental earthquake processes and temporal behavior, in addition to aiding our site-specific seismic hazard characterizations.

Earthquake geology and seismology can provide complementary datasets in both theoretical and applied settings. For example, recent analysis of the distribution and style of Quaternary faulting in the Alaska Range (Bemis, 2010) demonstrate that the Denali fault is strongly strain-partitioned, and thus the prevailing model of interior Alaska seismicity being driven by dextral shear between the Denali and Tintina faults (Page et al., 1995) is not valid. Studies of active faults will benefit from increased resolution of the frequency and location of earthquakes, contributing to the determination of subsurface fault geometries that are fundamental for the calculation of fault slip rates. And both disciplines are required to understand the difference (if the difference is real) between the fault zones that produce abundant background seismicity vs. those that do not.

Bemis, S.P., 2010, Moletrack scarps to mountains: Quaternary tectonics of the central Alaska Range [Ph.D.]: University of Oregon.

Page, R.A., Plafker, G., and Pulpan, H., 1995, Block rotation in east-central Alaska: A framework for evaluating earthquake potential?: *Geology*, v. 23, no. 7, p. 629-632.

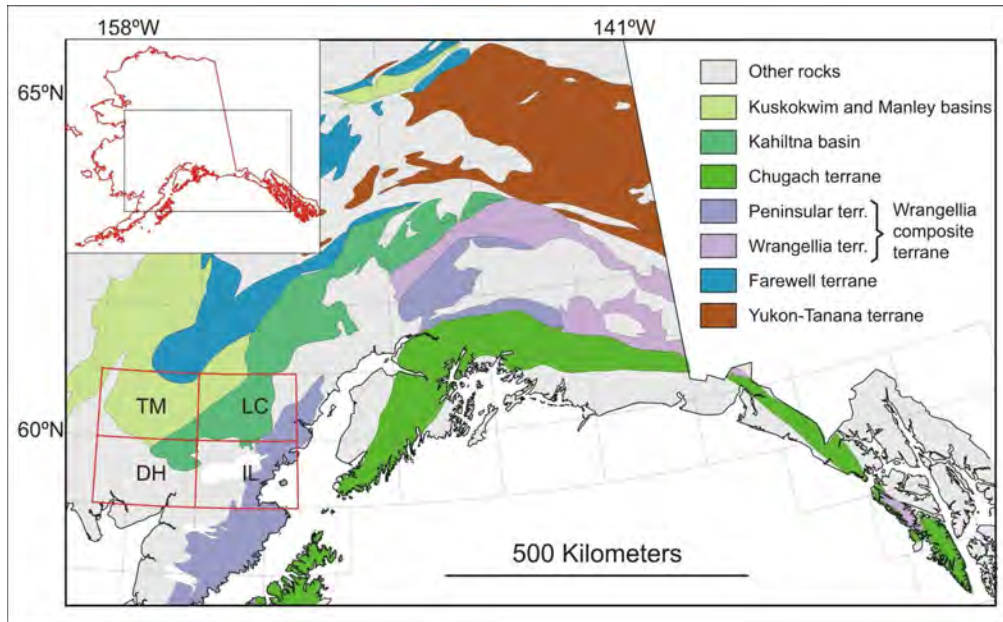


Fig. 1. Terrane map of southern Alaska from Bradley et al. (2006). USGS geophysical studies in Alaska in support of concealed mineral resource assessment fall within the four highlighted map sheets.

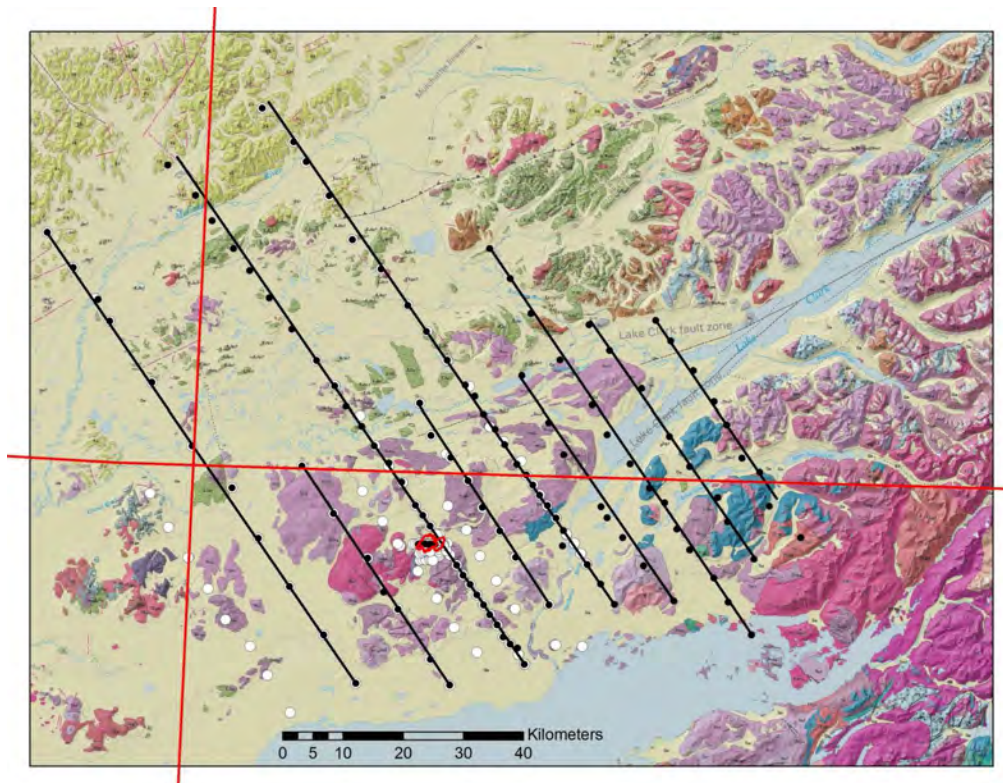


Fig. 2. USGS Geophysics in southwestern Alaska including magnetotelluric (black) and gravity (white) stations. The Pebble Cu-Au-Mo porphyry deposit is outlined in red. Geology from Wilson et al. (2006).

University of Alaska Geochronology Facility: Ongoing collaborations on the rock record of Neogene deformation in southern Alaska.

Jeff Benowitz¹, Paul Layer², Sean Bemis³, Sarah Roeske⁴

¹Department of Geology and Geophysics, University of Alaska, Fairbanks
jbenowitz@alaska.edu

²College of Natural Science and Mathematics, University of Alaska, Fairbanks
pwlayer@alaska.edu

³Sean Bemis, Geology Department, University of Kentucky
sean.bemis@uky.edu

⁴Presenter Geology Department, University of California, Davis
smroeske@ucdavis.edu

Abstract:

The planned EarthScope deployment of the USArray in Alaska provides exciting opportunities for understanding mantle-crust interactions in a complex convergent margin. An ongoing wide-spread GPS and EarthScope seismic instrument campaign will provide valuable insights into how stress from the ongoing flat-slab subduction of the Yakutat microplate at Alaska's southern margin is distributed inboard. Far-field response to the plate boundary coupling is expressed as both vertical and horizontal tectonics along crustal-scale faults such as the Denali Fault system. Results from this study will have both regional and broad scale tectonic implications. In particular, results from this project will help define what constitutes the boundaries of blocks of Alaska crust, and whether the wide plate boundary zone between the Pacific and North American plates is best characterized by diffuse deformation, block rotation, or both. Results will also have relevance to how surface processes and seasonal hydrological changes affect vertical movement of the upper plate.

The deployments will also present an opportunity to integrate short term observations (e.g. GPS measurements) with Alaska's million year time scale tectonic history preserved in the rock record. The University of Alaska Fairbanks geochronology facility is currently involved in numerous collaborations in southern Alaska using thermochronology and geochronology integrated with micro- and macrostructural analysis to document continental-scale fault movements, block formation, block boundaries and block history, interactions between tectonic and glacial processes, and vertical tectonics. Recent projects have concluded that flat-slab subduction has influenced the tectonics of south-central Alaska for at least ~24 Ma, which is documented in the Neogene formation of the eastern Alaska Range and strike-slip movement along the eastern Denali Fault system. A central focus of our group's research is to investigate if particular regions of Alaska are undergoing diffuse/distributed deformation or are acting more block-like. Continuing and proposed projects along this front relevant to the EarthScope community include, but are not limited to:

- a) How do near-field structural irregularities like the Denali Fault restraining bend affect vertical tectonics (e.g. Mount McKinley) and is there a rock record of southern Alaska block movement history along the Denali Fault restraining bend?
- b) Why does the slip rate of the Denali fault vary along strike, and do these rates change through time?
- c) Does the rock record of the western Alaska Range support the inference of a boundary between the Bering and southern Alaska blocks?
- d) In the Talkeetna Mountains, is there a record of south to north Neogene progressive exhumation related to the location of the Yakutat flat slab through time?
- e) Do active faults and glacial processes, through an unique feedback system, magnify the effect both processes have on the long-term erosion history of a region?

We look forward to discussing these current projects with the EarthScope community and avenues for integrating the objectives of the USArray with our work. We also look forward to discussing further collaborations integrating the modern and geological record.

CRUSTAL STRUCTURE OF THE CENTRAL ALASKA RANGE

Patrick Brennan, Hersh Gilbert and Ken Ridgway • Purdue University

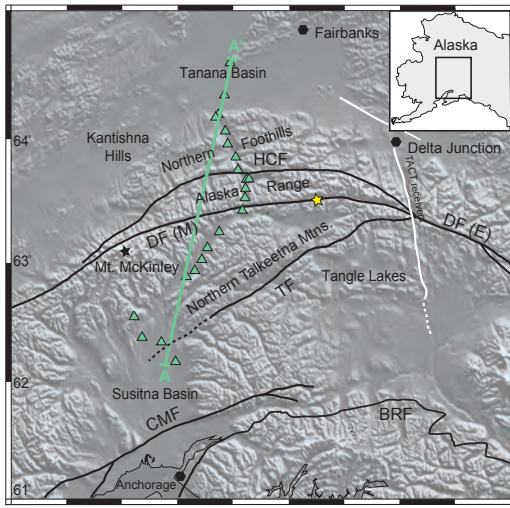


Figure 1. Shaded relief map of the study area showing receiver function transect line, seismic station locations, and major fault systems. Green triangles indicate stations used in this study. Up-right triangles indicate stations from the BEAAR temporary deployment, upside-down triangles indicate permanent seismic stations of the AEIC. The location of the TACT transect is shown by the white lines. Major faults are outlined by heavy black lines, DF (M) = McKinley fault, HCF = Hines Creek fault, TF = Talkeetna fault, DF (E) = Eastern Denali fault, CMF = Castle Mountain fault, BRF = Border Ranges fault. Yellow star shows the location of the M 7.9, 2002 Denali earthquake. The black star shows the location of Mt. McKinley (Denali) that has an elevation of 6194 m. Major towns are shown by black polygons. Modified from Brennan et al. (2011).

The growth of continents through the collision and accretion of terranes, such as oceanic plateaus and volcanic arcs, has been recognized as a fundamental and first-order tectonic process. The welding process of terrane accretion leads to the development of a suture zone between the former continental margin and the allochthonous body. Although suture zones represent syn-collisional features they may also act as potential zones of reactivation, the long-term growth of continents therefore effectively seeds the crust with inherently weak zones. The central Alaska Range presents an ideal location to study the crustal structure of a collisional zone as its part of a regional suture that extends from British Columbia to southwestern Alaska and the well-exposed surface geology documents a clear transition from oceanic to continental crust.

Preliminary insights on the crustal structure of the Mesozoic Alaska Range suture zone are observed from receiver function transects across the central Alaska Range (Fig. 1, 2). Observations of crustal thickness, intra-crustal discontinuities, and V_p/V_s allows for the identification of three distinct crustal sections: a southern section that is ~30 km thick and has a more mafic composition; a central section that is ~37 km thick that

exhibits several intra-crustal discontinuities and has felsic to intermediate composition; and a northern section with ~27 km thick crust of felsic to intermediate composition (Fig. 2). We interpret these sections to correspond to the allochthonous oceanic terrane (Wrangellia composite terrane), the suture zone proper, and the former continental margin (Yukon composite terrane), respectively. The boundary between the Wrangellia composite terrane and the suture zone appears to be a relatively discrete, near-vertical boundary (Fig. 2). The boundary between the suture zone and the Yukon composite terrane, however, appears to be a subhorizontal discontinu-

ity (Fig. 2). This discontinuity may have accommodated underthrusting of suture zone crust beneath the former continental margin, resulting in the 'doubled Moho' signature observed here (Fig. 2). Observed variability in the bulk composition of the three sections has likely influenced the observed differences in crustal structure between the sections. Compositional variations between the components of the suture zone likely influence how these regions respond to pre-, syn-, and post-collisional deformation. The crustal character of accreted terranes along continental margins will likely influence the long-term distribution of deformation.

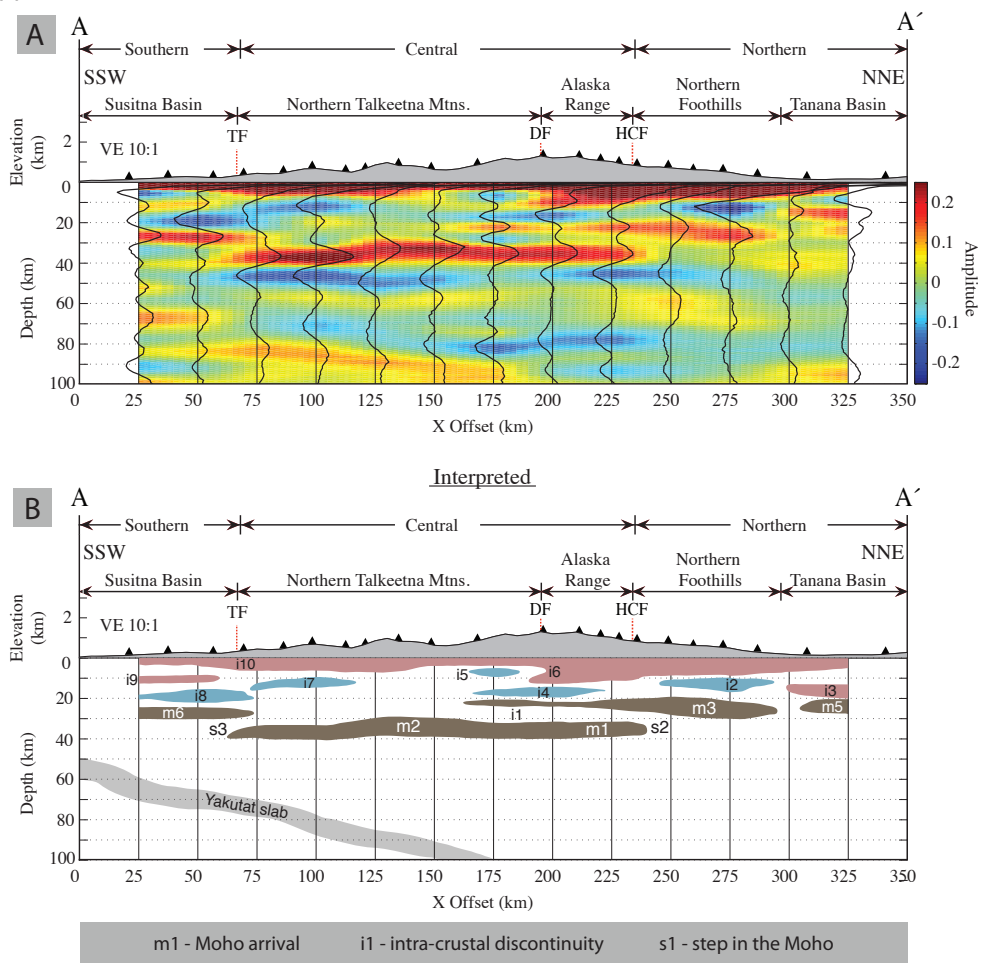


Figure 2. CCP stacked receiver function (1.2 Hz frequency) transect along cross-section A-A, simplified interpretations of the stacked receiver function transects are shown below the transect. A) CCP stacked receiver function transect along transect A-A'. Positive arrivals are shown as red whereas negative appear as blue. Stacked receiver functions for each column of CCP bins are shown by solid black lines. The topographic profile is averaged for a 10 km swath parallel to the line of transect and is shown 10 times vertically exaggerated. Regions discussed within the text are shown above the cross-sections, as are major fault crossings. TF = Talkeetna fault, DF = Denali fault, HCF = Hines Creek fault. Distance along the transect is shown by x offset from the southern endpoint of the transect (A-A'). See text for discussion. B) Interpreted CCP stacked receiver function transect A-A'. The interpreted transect is presented below the CCP stacked receiver transect for comparison to the data. The major arrivals are shown by colored polygons, which emphasize the geometry, extent, and depth of the arrivals. The Moho conversions are shown by brown polygons and are labeled m followed by a number. Intra-crustal discontinuities are red (corresponding to positive arrivals) or blue (corresponding to negative arrivals) and labeled with an i followed by a number. The steps in the Moho are labeled with an s followed by a number. The individual interpretations are discussed in the text. The simplified profile of the subducting Yakutat plate is shown by the gray polygon. From Brennan et al. (2011).

References cited: Brennan, P. R. K., H. Gilbert, and K. D. Ridgway (2011), Crustal structure across the central Alaska Range: Anatomy of a Mesozoic collisional zone, *Geochem. Geophys. Geosyst.*, 12, Q04010, doi:10.1029/2011GC003519.

Prehistoric tsunami deposits and megathrust-related land-level changes on Chirikof Island, Aleutian subduction zone

Richard Briggs¹, Alan Nelson¹, Guy Gelfenbaum², Simon Engelhart³, and Tina Dura³

¹ US Geological Survey, Golden, Colorado

² US Geological Survey, Menlo Park, California

³ Department of Earth and Environmental Science, University of Pennsylvania

Chirikof Island lies near the eastern end of a section of the Aleutian megathrust that ruptured during great earthquakes in 1788 and 1938. Historical accounts suggest that the 1788 earthquake generated a large tsunami, and tsunami propagation models predict that a 1788-style rupture on the Aleutian megathrust will direct its maximum energy toward the west coast of the contiguous United States. Fournier and Freymueller (2006) used GPS geodesy to show that the 1788 rupture patch is highly coupled beneath Chirikof Island and that significant coupling extends to the west through the Shumagin Islands. These observations motivated our research on Chirikof Island in August 2010 to: (1) demonstrate the potential for identifying and dating the deposits of prehistoric tsunamis on Chirikof Island and elsewhere in the eastern Aleutians, (2) investigate evidence for megathrust-related land-level changes on Chirikof Island, and (3) develop a scientific and logistical framework for future studies of prehistoric tsunamis and earthquakes in the Aleutian region.

We described stratigraphic evidence for prehistoric tsunami deposits in the freshwater marshes of Chirikof Island (Figure 1a). Nearly 40 reconnaissance gouge cores and four 2 to 5-m-long Russian cores (13 m total length) were obtained from low-lying basins in the southwest part of the 11-by-17-km island (Figure 1b). Site TR, a 250-m-wide basin 11 m above present sea level, is filled with at least 5 m of freshwater peat deposited over the past 12,000 years. Preliminary AMS radiocarbon ages date a 5 to 15-cm-thick sand bed overlying two distinct tephras to 10.5 ka and three 0.5 to 2-cm-thick sand and silty-sand beds separated by 1-3 cm of peat to about 4.0 ka (Figure 1c). Considering their 11 m elevation, these and at least one other sandy bed in the peat sequence are almost certainly tsunami deposits. At site RR, we cored a 4000-yr-old, 4+ m thick sequence of freshwater peat that extends up a 50-m-wide valley between 7-15 m above sea level. As many as 14 beds of sand, silty sand, and silty peat occur between an upvalley sedimentation zone dominated by stream and debris-flow deposits and a downvalley area where eolian sands and storm deposits occur. We are conducting grain-size distribution analyses and preparing microfossil samples, including diatoms and pollen, to distinguish between tsunami, storm surge, and eolian origins for each of these sandy beds. One of five closely spaced sandy beds in the upper 0.5 m of the sequence was likely deposited by the 1788 tsunami.

We identified the geomorphic signature of megathrust-related land-level changes along the Chirikof coast. Geomorphic mapping, aided by high-resolution satellite imagery, historical airphotos, and RTK GPS surveys tied to National Oceanographic Service (NOS) benchmarks, documents the landward progression of beach features as Chirikof subsides in the interseismic period (Figure 1b). Based on the locations of rapidly eroding archeological sites and our mapping of coastal features, we infer that coseismic uplift during megathrust events is nearly completely recovered interseismically and that net late Holocene emergence is negligible. A cobble beach berm, probably abandoned during previous coseismic uplift of the island, is a datum showing that the island has subsided to within a few decimeters of its elevation prior to previous sudden uplift (Figure 1d). These geomorphic observations are consistent with continuous GPS data from the Plate Boundary Observatory (PBO) station AC13 on Chirikof, which shows subsidence of ~10 mm/year.

Our 2010 data provides a baseline for further work in the region, which we will compare with records of prehistoric earthquake-induced land-level changes and tsunamis on Kodiak Island, 125 km to the northeast. In summer 2011 we will extend this study to Simeonof Island in the outer Shumagin Islands, 250 km southwest of Chirikof Island. On Simeonof, freshwater bogs and marshes may record paleotsunamis, and elevated and abandoned constructional beach features may reflect internal deformation of the upper plate and coupling along the underlying subduction interface. Constructing a history of great megathrust earthquakes and their accompanying tsunamis in this part of the Aleutian Arc will help us better understand the tectonic behavior of this plate boundary as well as assess earthquake and tsunami hazards.

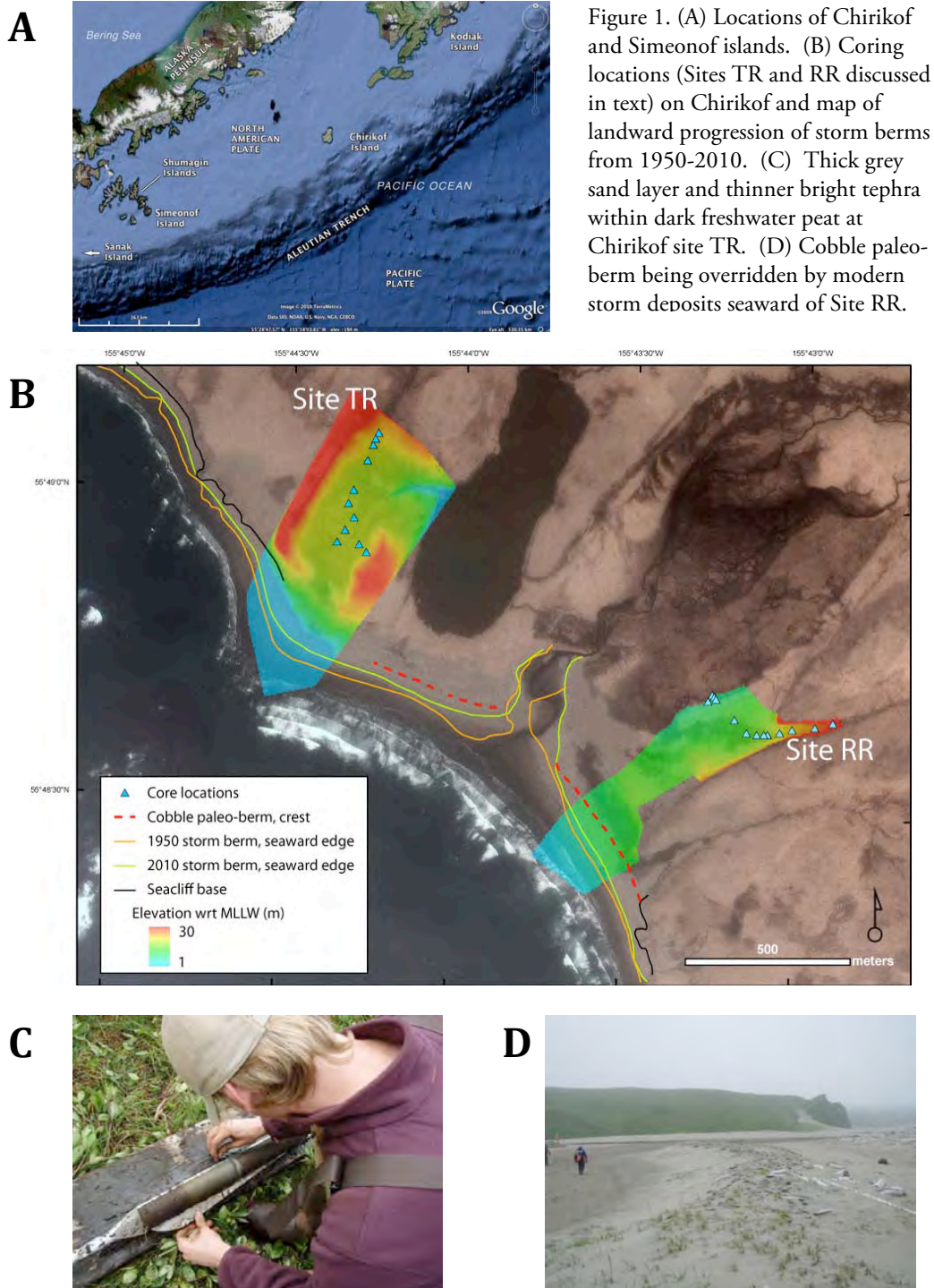


Figure 1. (A) Locations of Chirikof and Simeonof islands. (B) Coring locations (Sites TR and RR discussed in text) on Chirikof and map of landward progression of storm berms from 1950-2010. (C) Thick grey sand layer and thinner bright tephra within dark freshwater peat at Chirikof site TR. (D) Cobble paleo-berm being overridden by modern storm deposits seaward of Site RR.

Using the earthquake simulator RSQSim as a tool investigate subduction zone processes

By: Harmony V. Colella and James H. Dieterich

The Alaska-Aleutian Subduction Zone is a natural laboratory to investigate the interactions between unstable, transitional, and stable slip. The historical occurrence of great mega-thrust earthquakes and the recent identification of slow slip events (SSEs) along the Alaska-Aleutian Subduction Zone demonstrate slip variability both along strike and along dip. These observations raise important questions: How might the different sliding processes interaction with one another along the subduction interface, and to what extent do these interactions affect probabilities of great Alaska-Aleutian mega-thrust earthquakes?

The earthquake simulator, RSQSim, is currently being employed to investigate similar questions along the Cascadia Subduction Zone. RSQSim is a boundary element code that incorporates rate- and state-dependent constitutive properties to set different slip modes. It is computationally efficient, which permits long histories with a wide range of event sizes to generate synthetic statistical distributions of earthquakes and SSEs. Preliminary results yield average slip, recurrence intervals, durations, and propagations speeds that are in broad agreement with observations in Cascadia (Figure 1). These results provide confidence this simplified model captures several properties of the subduction zone interface. Additionally diverse slip propagations speeds and directions (Figure 2) (i.e. back propagation parallel to the slip front and along dip propagation perpendicular to the slip front) generated by the model are similar to those observed in nature (i.e. RTRs and tremor streaks).

Current and future data collected by EarthScope for the Alaska-Aleutian Subduction Zone can be used to complement these simulations. Models can be further refined in collaboration with geological and geophysical studies to more accurately replicate observations. Results may provide details regarding the physical conditions necessary to create the slip variability observed along strike and along dip of the subduction zone interface. Additionally, simulations may capture details that can be used to guide geological and geophysical observations.

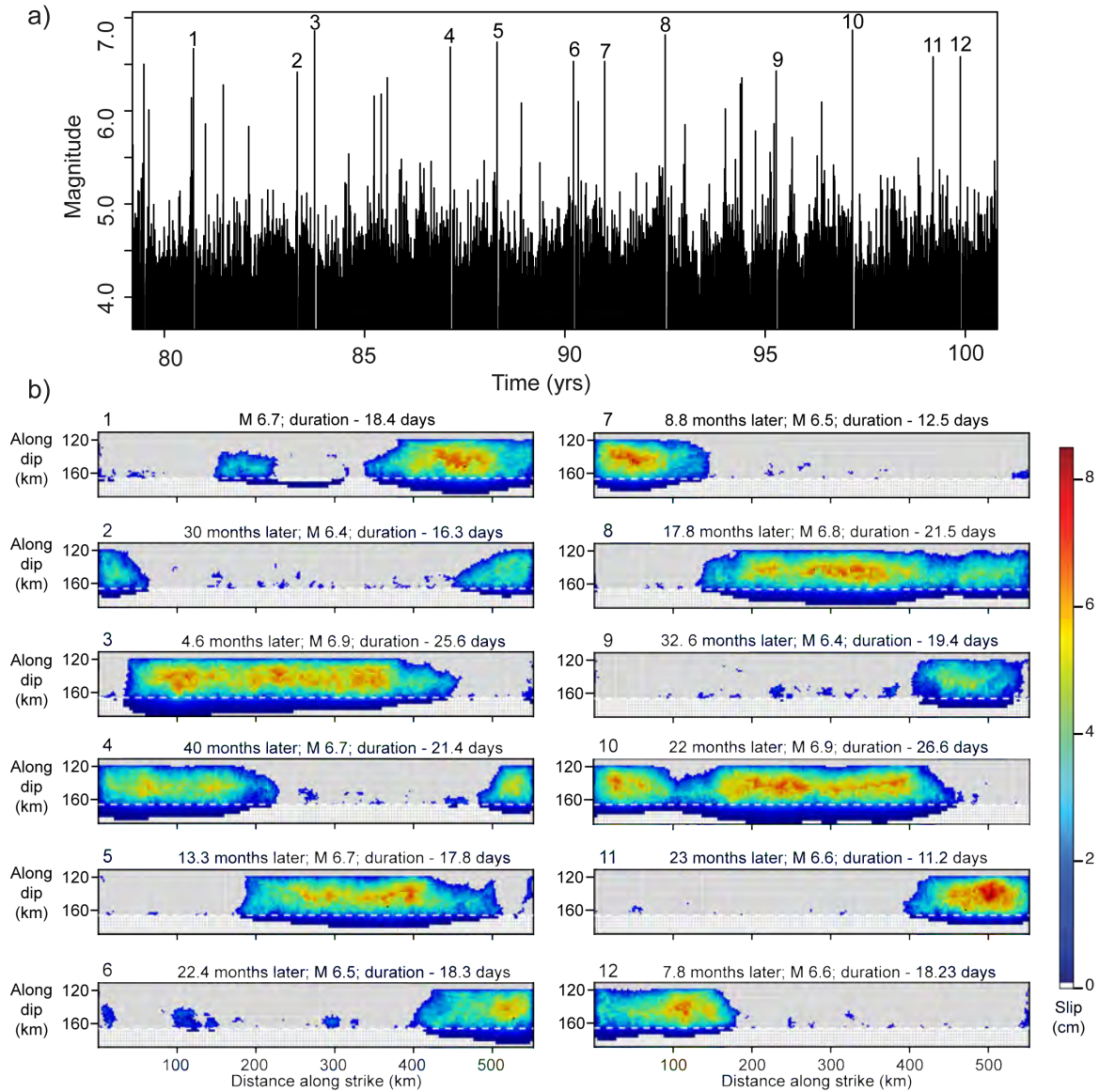


Figure 1: 22 years of SSEs from the simulation. b). Slip distribution for a sequence of $M_w > 6.4$ SSEs, where events correspond with those noted in 1a. Note the penetration of slip into the continuous creep zone.

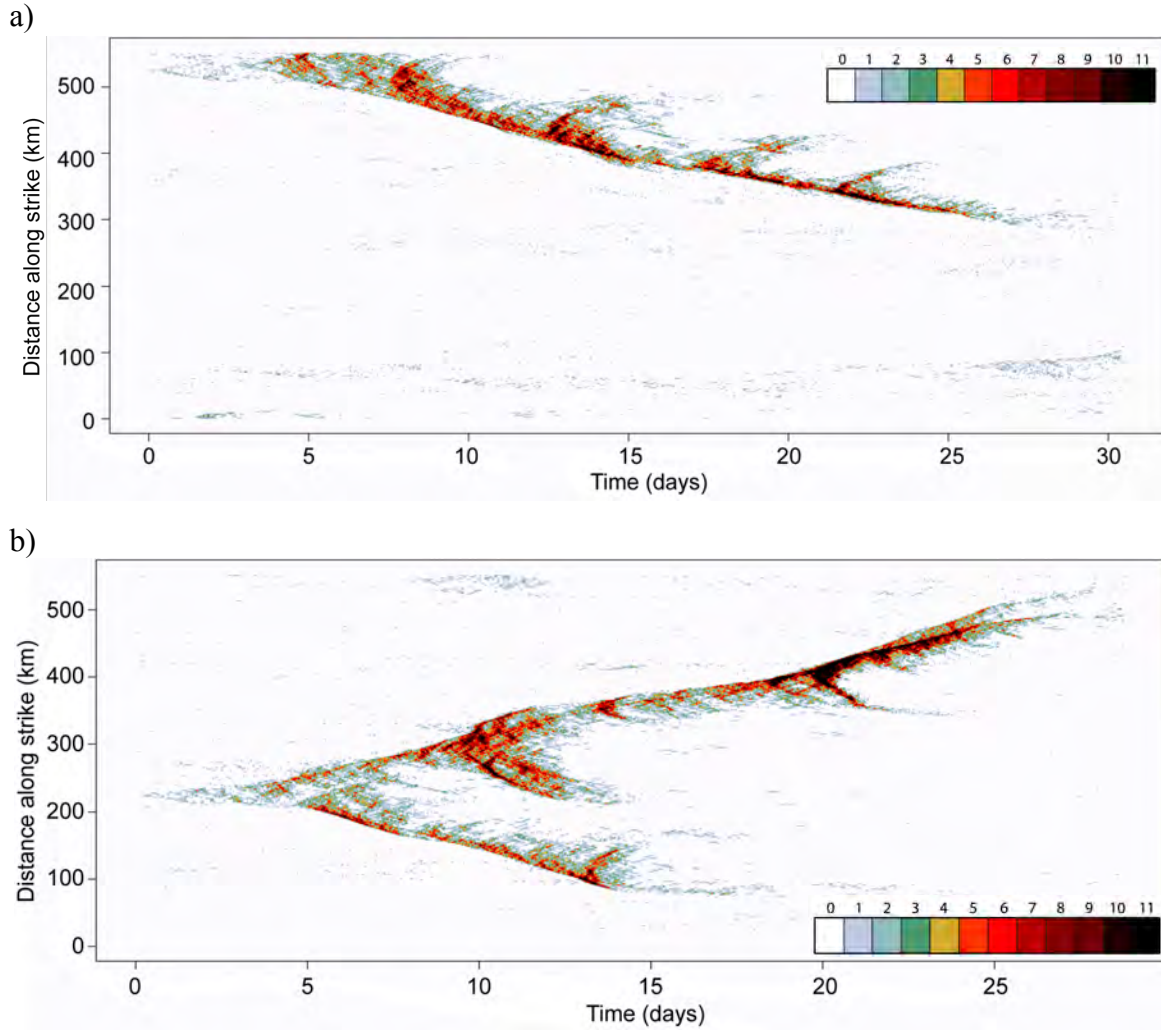


Figure 2: Space-time evolution of slip during simulated SSEs. Colors correspond to the number of patches along dip that slip at a given time. a). Example of unilateral propagation. b) Example of bilateral propagation.

Integrated Interpretation of Potential Fields and Seismicity Data to Constrain Earthquake and Tectonic Processes in Alaska

Diane Doser, Niti Mankhemthong, and Hugo Rodriguez, Department of Geological Sciences, University of Texas at El Paso, El Paso, TX 79968 (doser@utep.edu)

We have been using land and marine gravity and aeromagnetic data to examine structural controls on shallow (< 20 km) and deeper seismicity within interior, southeast and south-central Alaska. Potential fields data were obtained from existing US and Canadian data bases, as well as gravity data acquired from recent (2009-present) field campaigns in south-central Alaska. Comparisons of these data to relocated seismicity indicate a number of intriguing features.

In south-central Alaska shallow (<30 km) seismicity within Cook Inlet lies within a -75 mGal Bouguer anomaly low and magnetic high that may be related to a mid-crustal serpentinite body. In contrast, little deeper (> 30 km) seismicity occurs below this anomaly, with the thickest portion of the seismogenic zone lying south of the low. East of the Border Ranges fault (BRF) we observe a Bouguer anomaly high (> -50 mGal) throughout most of the eastern Kenai Peninsula, but a low (< -70 mGal) on the eastern side of the BRF east of Anchorage. We believe this change in gravity may reflect the subduction of the less dense Yakutat microplate north of Turnagain Arm.

In the Prince William Sound region shallow (< 15 km) seismicity occurs at the edges of mafic and ultramafic bodies that are delineated at depth by aeromagnetic highs. The edges of the strongly coupled Prince William Sound asperity correlate well with the edge of the -20 mGal Bouguer anomaly associated with the shallowly dipping Yakutat microplate and Pacific plate beneath the region.

In southeastern Alaska, offshore aeromagnetic anomalies correlate well with segmentation of the Queen Charlotte fault system, while onshore limited gravity observations suggest Fairweather fault segmentation is controlled by basement geology. A Bouguer gravity high (> 30 mGal) is associated with maximum moment release during the 1958 Fairweather earthquake. In the Yakutat region the intersection of the Pamplona fault zone with the northeastern edge of the Yakutat microplate and the Chugach-St. Elias fault system is marked by a Bouguer anomaly high with seismicity concentrated at the northwest and southeast edges of the high. Similar structural controls for rupture in $M > 7$ earthquakes are indicated by potential fields data in interior Alaska.

It is obvious that potential field data can greatly enhance our understanding of structural controls on the earthquake rupture and subduction processes. Unfortunately, gravity and magnetic data are sparse in many regions of Alaska, and existing data were often collected several decades ago with lower resolution instrumentation and less precisely determined station locations. We urge that potential field data, especially gravity, be collected, when possible, in tandem with other Earthscope activities, such as site installations.

GPS Constraints on Active Deformation in Southern Alaska and the Role of the Yakutat Block

A White Paper Prepared for the “Opportunities for Earthscope Science in Alaska” workshop held in advance of the 2011 Earthscope National Meeting

Julie Elliott, Jeff Freymueller, and Chris Larsen – University of Alaska Fairbanks

Data from a network of predominately campaign GPS sites in southern Alaska and the northern Canadian Cordillera have helped to redraw our picture of the region’s tectonics. Instead of a comparatively simple interaction between the Pacific and North American plates, with relative motion accommodated on a single boundary fault, the GPS velocity field reveals a margin made up of a number of small blocks and deformation zones with relative motion distributed across a variety of structures. Much of this complexity can be attributed to the Yakutat block, an allochthonous terrane that has been colliding with southern Alaska since at least the Miocene.

In southeast Alaska, a GPS-derived model shows that the surface deformation can be largely explained in terms of block motion. The Yakutat block is predicted to move NNW at a rate of 50 mm/a, a velocity that is similar in magnitude but more westerly than that of the Pacific plate. Along its eastern edge, the Yakutat block is deforming, resulting in margin-normal convergence outboard of the Fairweather-Queen Charlotte fault system. That dextral fault system accommodates the majority of the relative plate motion in southeast Alaska with slip rates of 40 – 45 mm/a. Part of the strain from the Yakutat collision is transferred east of the Fairweather – Queen Charlotte system, causing the region inboard of the Fairweather fault to undergo a distinct clockwise rotation into the northern Canadian Cordillera. Further south, the region directly east of the Queen Charlotte fault displays a much slower clockwise rotation, suggesting that it may be at least partially pulled along by the northern block motion. About 5% of the relative motion is transferred even further east and results in small northeasterly motions well into the northern Cordillera.

The predicted Yakutat block velocity results in ~ 45 mm/a of NW-directed convergence with southern Alaska. Based on the GPS velocity field, the western edge of the Malaspina Glacier marks the northwestern boundary of the Yakutat block and main deformation front between the two blocks. Multiple narrow, northwesterly moving blocks bounded by N- to NW-dipping thrust faults are required to explain the observed surface deformation north of the collision front. These “blocks” may be more aptly termed crustal slivers or deformation zones due to their size and because their bounding faults likely sole out into a decollement. Slip on a combination of three faults between the deformation front and Mount St. Elias accommodates ~ 75% of the relative convergence.

The shallow crustal faulting surrounding the collision front continues west until the vicinity of the Bering Glacier, where a northward rotation and increased magnitudes in the GPS velocity field indicate a transition from collision and accretion to subduction of the Yakutat block. This transition lies almost due north of the Gulf of Alaska Shear zone, suggesting that the northern Pacific plate is fragmenting in response to the Yakutat collision. Variations in coupling along the Yakutat – Southern Alaska subduction interface are observed, with a region of lower coupling occurring around Cordova in eastern Prince William Sound.

Estimation of Basal Tractions Acting at the Base of the Lithosphere Beneath Alaska and northwestern Canada

Emily Finzel*, Lucy Flesch, and Ken Ridgway

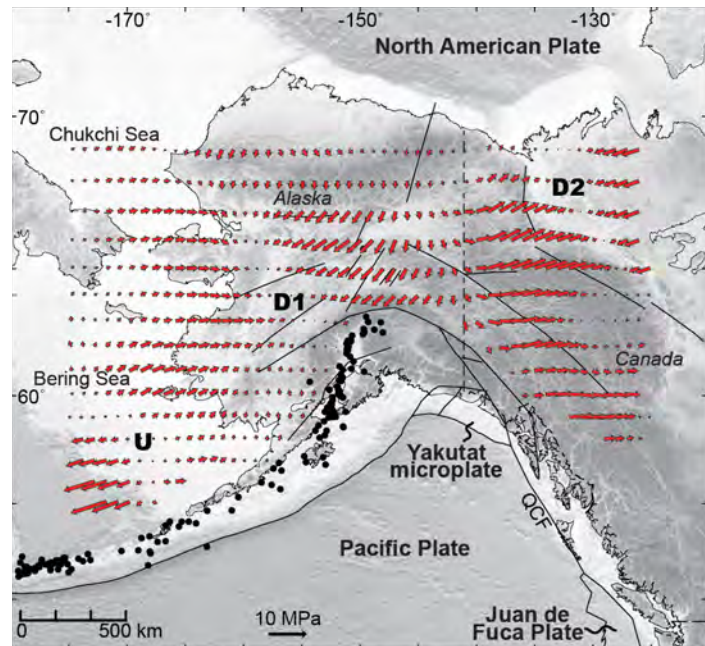
Department of Earth and Atmospheric Sciences, Purdue University

*Now at ExxonMobil Exploration Company

There are three proposed lithospheric-scale driving forces for continental deformation at convergent margins: 1) boundary forces related to plate motions, 2) buoyancy forces related to lateral deviations in gravitational potential energy (GPE) associated with variations in lithospheric thickness, and 3) basal tractions generated by mantle flow. The discrete contributions that these three forces make to the stress tensor field in western Canada and Alaska have not been quantified in detail, so their relative role in influencing deformation has remained unresolved. We have used dynamic models to calculate preliminary estimates of deviatoric stresses associated with both gradients in GPE and first order stress boundary conditions (plate motions).

In addition, we have calculated estimates of the forces applied to the base of the lithosphere associated with tractions from large-scale mantle flow. We investigate the role of tractions acting at the base of the lithosphere by

looking at the difference between the observed deformation fields inferred from GPS observations and geologic data (kinematic model) and deformation fields produced in self-consistent dynamic models. The kinematic deformation fields presumably contain the response from variations in Gravitational Potential Energy (GPE), relative plate motions and tractions acting along the base of the lithosphere. The self-consistent dynamic solution is driven by lithospheric density variations and the kinematic velocity boundary conditions that contain the integrated effect of tractions associated with large-scale mantle flow up to the boundary of the grid. However they do not contain the contribution from basal tractions acting at the base of the grid. Therefore, the difference tensor fields between the kinematic and dynamic models reflect the response to basal traction, if the GPE estimates are accurate (e.g., accurate lithosphere structure model), and to lesser extent if the relative effective viscosities are reasonably well resolved.



Forces acting at the base of the lithosphere calculated from the difference in strain rate fields between an observed kinematic strain rates determined from the interpolation of GPS and Quaternary faults and geodynamic modeled strain rates driven by gradients in gravitational potential energy, variation in lithospheric strength, and velocity boundary conditions. Thus, the difference between the two fields should represent the contribution of basal tractions in driving deformation in Central Alaska. U-zone of upwelling, D1/D2-zones of downwelling.

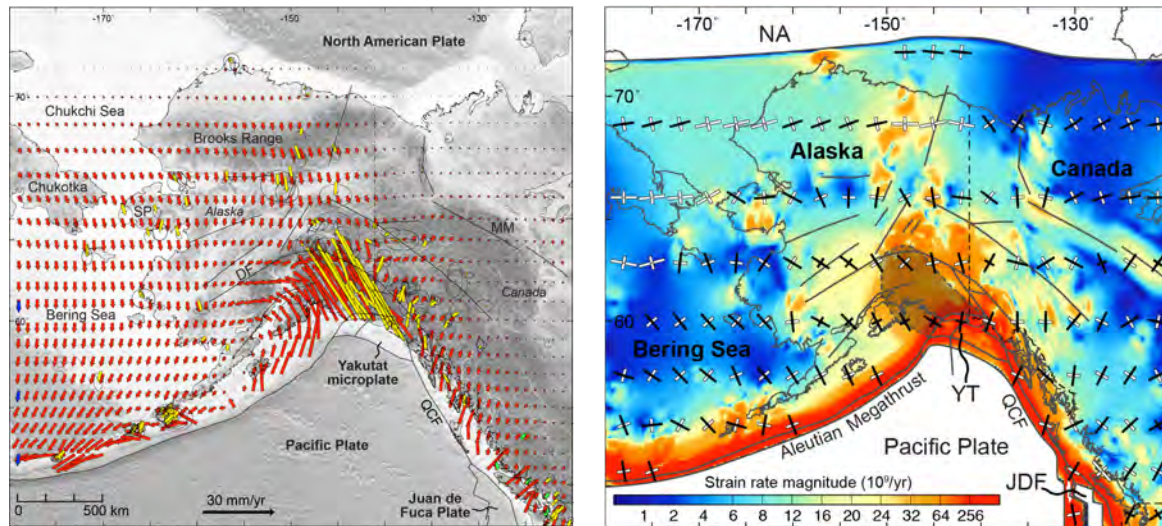
Kinematics of a Diffuse North America-Pacific Plate Boundary Zone in Alaska and Western Canada

Emily Finzel*, Lucy Flesch, and Ken Ridgway

Department of Earth and Atmospheric Sciences, Purdue University

*Now at ExxonMobil Exploration Company

Regional kinematic models of Alaska and western Canada are limited to those based on rigid microplates, which are inconsistent with the pervasive seismicity in the region, or were developed before the availability of Global Positioning System (GPS) data. A major unanswered question in the modern plate tectonic configuration of Alaska is the extent of the enigmatic Bering plate and its role in the neotectonic deformation field. We provide a synoptic analysis of the kinematics and neotectonics of Alaska and western Canada, and in particular addresses the location and nature of the present day plate boundaries in the region. We use numerical finite element models that are constrained by observations of long-term strain rates, including plate and microplate motion models, ridge spreading rates, seismicity, and Quaternary fault slip rates, as well as recently released GPS data that have not previously been used to model the region, to produce a continuous velocity and strain rate field. Our results have several important implications in Alaska and western Canada: 1) non-rigid accommodation of deformation is an important mechanism and is required in any kinematic model of the region; 2) tectonic extrusion likely does not play an important role in the current kinematics; 3) the relative motion between the Pacific and Bering plates may be a governing driver in the neotectonics of the region; and 4) the North America-Pacific-Bering plate boundary is a far-reaching zone of diffuse deformation that extends for more than 1000 km across Alaska.



(left) Modeled continuous horizontal velocity field (red vectors). Yellow vectors are GPS observations, green vectors represent motions of various blocks defined in that region (McCaffrey et al., 2007), and create a Bering plate boundary condition along the western boundary (Freymueller et al., 2008). DF-Denali fault; QCF-Queen-Charlotte Fault; SP-Seward Peninsula; MM-Mackenzie Mountains; V-Valdez; N-Cantwell. (right) Modeled continuous strain rate field. Bars show normalized horizontal principal contractional (black) and extensional (white) strain axes. Strain rate magnitude is shown in the background grid. Inferred subducted extent of the Yakutat microplate is shown by dashed line (modified from Eberhart-Phillips et al., 2006)

Implementation of temporary Earthquake Early Warning and improved Tsunami Warning for Alaska.

White paper for the 'Opportunities for EarthScope Science in Alaska in Anticipation of USArray' Workshop

Ronni Grapenthin, Geophysical Institute, University of Alaska Fairbanks, ronni@gi.alaska.edu

Alaska has enormous seismic potential; over the last 100 years several earthquakes with magnitudes $M > 8.0$ ruptured along the Alaskan subduction zone, including the $M=9.2$ Great Alaska earthquake of 1964. Given that Alaska is now more densely populated than it used to be and more people live along the Pacific coast, a reliable earthquake early warning and tsunami pre-warning system must be implemented to save lives and property. In doing so we should learn from the 11 March 2011 $M=9.0$ Tohoku-oki earthquake. This event was initially estimated at about $M=8.0$, some tsunami forecasts models saturate at this magnitude. Furthermore, we measured only co-seismic subsidence along Japan's east coast where we would usually also expect uplift due to elastic rebound of the plate. This affected the sea floor dynamics in unforeseen ways, contributing to an unexpectedly devastating tsunami.

The GPS displacement data of Japan clearly shows that about 3-4 minutes after rupture onset the co-seismic displacements of coastal Japan reached their maximum; at this time the S-waves and surface waves had not yet propagated through southern Japan. From the spatial pattern of these static displacements it was clear that (1) the event must be larger than initially estimated and (2) the tsunami will be much different in nature than anticipated as all of the uplift and likely some subsidence induced by the rupture located in the ocean. This information could have been available in near real time.

I suggest to make use of the dense instrumentation of Alaska during the time USArray will be deployed and supplement the already installed Plate Boundary Observatory GPS stations. Even if only temporary, the data generated during these deployments should be used in real time to constrain tsunami forecast models and realize earthquake early warning for heavily populated areas like Anchorage and industrious places that create a hazards to vulnerable (sub-) arctic ecosystems.

Before the arrival of USArray in Alaska, additional PBO station should be equipped for (temporary) real time streaming (only 7 now). Data of USArray and PBO should be merged and understood as displacements with respect to an average position of each site. For the GPS stations a network of stations away from the subduction zone must be identified to minimize the effect co-seismic displacements will have on the positioning solutions. This network of a few stations can be used as base stations to solve the position for the other PBO stations, assumed to be kinematic stations. These computations can be heavily parallelized as no kinematic site will constrain the position of another kinematic site. The USArray waveforms available in real time should be integrated into displacements; likely with respect to an average position. Once the cumulative displacements for the network are calculated the resulting time series must be analyzed with respect to their geographical position in the station network: a spatial smoothing algorithm should eliminate outliers, another algorithm should detect anomalous displacements at neighboring sites consistent with co-seismic displacements and issue the necessary alarms if applicable. Once the co-seismic displacements have stabilized they can be used to derive an expected magnitude (further constrained by expected displacements for historic earthquakes as identified using model runs, take seismic estimates into account); this magnitude and the displacement field are then handed to a tsunami forecast model which uses traditional seismic observations to further constrain the forecast. Realistically, the necessary computations are completed in near real time.

Constraining origin and delineating basement and upper crustal boundaries associated with accreted terranes in the Alaska Range suture zone, southern Alaska

Brian A. Hampton, Dept. of Geological Sciences, Michigan State Univ. [bhampton@msu.edu]

The neotectonic development of southern Alaska is largely the result of Neogene collision of the Yakutat terrane and the far-field effects of this event are observed across 100s of km throughout southern and interior Alaska. In anticipation of the EarthScope USArray, one particular region of interest in terms of strategic deployment is the Alaska Range suture zone of southern Alaska—a region up to ~100 km wide that occurs between the Wrangellia composite terrane (allochthonous island arc) and Yukon-Tanana terrane (peri-cratonic fragment of Laurentia) (Figure 1). The Alaska Range suture zone initiated as a result of the Mesozoic accretion of the Wrangellia composite terrane to the western margin of North America and consists largely of deformed Jurassic–Cretaceous synorogenic strata (Kahiltna assemblage) as well as a number of Paleozoic–Mesozoic tectonostratigraphic terranes (e.g. Farewell, Chulitna, McKinley-Windy) that are thought to have intraoceanic, circum-Arctic, or Laurentian origins.

The northern boundary of the suture zone in the Alaska Range is bounded by the Denali and Hines Creek faults and contains some of the highest topography in the North American Cordillera. The southern boundary of the suture zone roughly parallels the Talkeetna fault and Valdez Creek shear zone as well as the south Alaska magnetic high along the northern margin of Wrangellia. The central part of the suture zone is marked by a NE-SW trending lineament (Broad Pass) that separates the southern Alaska Range from the northern Talkeetna Mountains. The Broad Pass lineament corresponds roughly with sporadic outcrops of sheared serpentinite and ultramafic rocks that exhibit a distinct aeromagnetic anomaly throughout the central parts of the suture zone. Although the basement along the margins of the Alaska Range suture zone has been well documented, the origin, composition, and thickness of exposed Paleozoic–Mesozoic terranes as well as the overall response of the lithosphere to Yakutat collision throughout this region is largely unknown.

Recent U-Pb detrital zircon data from the central parts of the suture zone are beginning to reveal some insight into the origin of basement associated with some of these tectonostratigraphic terranes that occur between the Denali fault and Broad Pass aeromagnetic anomaly. One example from the southern Alaska Range is the Chulitna terrane which has long been considered as the type example of an exotic/suspect terrane that developed in an intraoceanic setting that was distinct from the North American Cordillera. However, new U-Pb detrital zircon ages from Upper Triassic strata of the Chulitna terrane document primary contributions Devonian–Mississippian magmatic source areas (peak ages of 336 and 342 Ma) and subordinate contributions from Triassic (peak ages of 205 and 212 Ma) and Silurian–Ordovician source areas (peak ages of 424 and 468 Ma), all of which are suggestive of a paleogeographic link with peri-Laurentian cratonic fragments of the outboard Cordilleran Intermontane belt. While these trends part with previously-interpreted origins for the Chulitna terrane, they also imply that the basement of the Chulitna and possibly other terranes in the central parts of the Alaska Range suture zone potentially consist of continental, transitional, or oceanic crust associated with the westernmost parts of the North American Cordillera (e.g. Stikinia and Yukon Tanana terrane).

In summary, ongoing provenance studies in the Alaska Range suture zone are providing new constraint on the origin of terranes as well as revised tectonic models on the basement and bounding structures that are adjacent to these terranes. A strategic approach to EarthScope USArray deployment in regions such as the Alaska Range suture zone may benefit from a focus not only on younger Mesozoic–Cenozoic features that bound the suture zone (e.g. Denali fault) but also on exposed Paleozoic–Mesozoic basement of select terranes that occur adjacent to continent-scale crustal structures throughout the Alaska Range and northern Talkeetna Mountains. Such an approach could provide much needed insight on the lithospheric stability of topographically highest parts of North America and further our understanding on how the Paleozoic–Mesozoic crustal elements in the northernmost parts of the Cordillera are responding to present day collision of the Yakutat terrane.

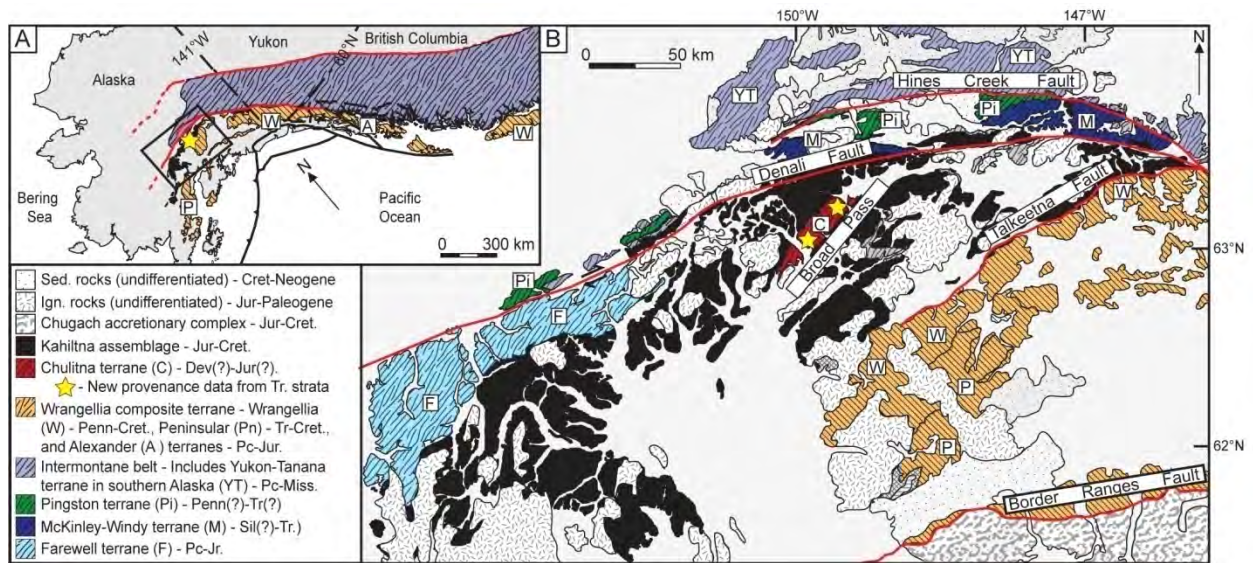


Figure 1. (A) Location map of the Alaska Range suture zone in the context of southern Alaska and the North American Cordillera. **(B)** Generalized geologic map of significant continent-scale structures (e.g. Denali fault) and Paleozoic–Mesozoic crustal elements that are exposed throughout the Alaska Range suture zone. Note that the suture zone is informally defined as the region between the Talkeetna fault and Hines Creek and Denali faults.

Testing and improving crustal velocity models of Cook Inlet, Alaska, through ambient noise correlations and seismic wavefield simulations

Matthew Haney¹, Carl Tape², Peter Haeussler³, and John Power¹

¹Alaska Volcano Observatory, U.S. Geological Survey, Anchorage, Alaska, USA

²University of Alaska Fairbanks, Geophysical Institute and Department of Geology & Geophysics, Fairbanks, Alaska, USA

³U.S. Geological Survey, Anchorage, Alaska, USA

The Cook Inlet is unusual compared to the rest of Alaska in that much is already known about the structure of the Earth's crust beneath it. This knowledge is the result of many years of oil and gas exploration in the Cook Inlet basin as well as nearby networks of seismometers used for long-term earthquake and volcano monitoring (Fig. 1). The basin is bounded to the east by the Border Ranges fault and reaches a maximum thickness of 7.8 km below the western edge of the Kenai Peninsula [1]. Understanding the amplification effect of the basin on seismic waves carries importance for the Cook Inlet given its earthquake activity and the fact that it is the location of over half the population of Alaska.

Within the field of seismology, it has recently been demonstrated that ambient noise recordings contain significant amounts of structural information, in particular for basins. This realization has resulted in many applications using correlations of ambient seismic noise recorded on pairs of seismometers [2–5]. For instance, the Hudson Bay [4] and Puget Sound area [5] basins have recently been imaged using ambient noise techniques, with resolution extending to sub-basin depths of 30–40 km. On a smaller scale, volcanic centers in Alaska have been imaged with ambient noise [3]. The interaction of the oceans and the solid Earth provides the noise source. For this reason, Alaska is well-suited for ambient noise techniques since storms in the Gulf of Alaska and the Bering Sea produce considerable levels of microseismic noise.

Shown in Fig. 2 are ambient noise correlations between station pairs within the network at the Katmai cluster of volcanoes, located south of the Cook Inlet on the Alaska Peninsula. The correlations in Fig. 2 clearly show a seismic surface wave, the Rayleigh wave, propagating between the stations. The observed speed of the surface wave contains information on the shear wave velocity in the crust. It turns out that this wave speed is frequency dependent - this is why the correlations in Fig. 2 have been bandpass filtered at 0.3 Hz. Observations of the surface wave speed over a wide frequency band leads to a 3D image of the crust, through the application of ambient noise tomography. In the case of basin-scale ambient noise imaging [4, 5], the frequency band of interest lies between 0.03 and 0.25 Hz. For volcanoes, Masterlark *et al.* [3] used frequencies between 0.2 and 0.7 Hz. Thus, the difference between basin-scale

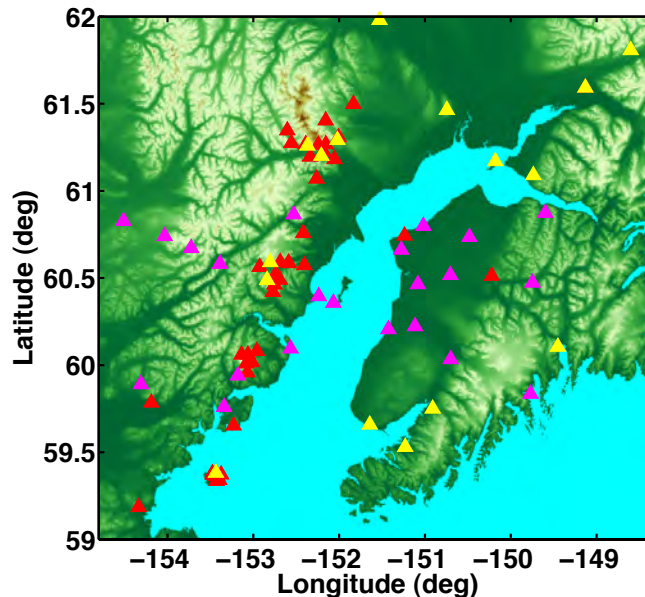


FIG. 1: Permanent stations from the AVO, AEIC, GSN, and WCATWC networks in and around Cook Inlet. Broadband stations are shown in yellow with short period instruments in red. A proposed Earthscope Flexarray deployment, consisting of 22 broadband stations and shown by magenta triangles, is intended to fill the gaps in the current coverage and facilitate the use of ambient seismic noise to probe the basin structure.

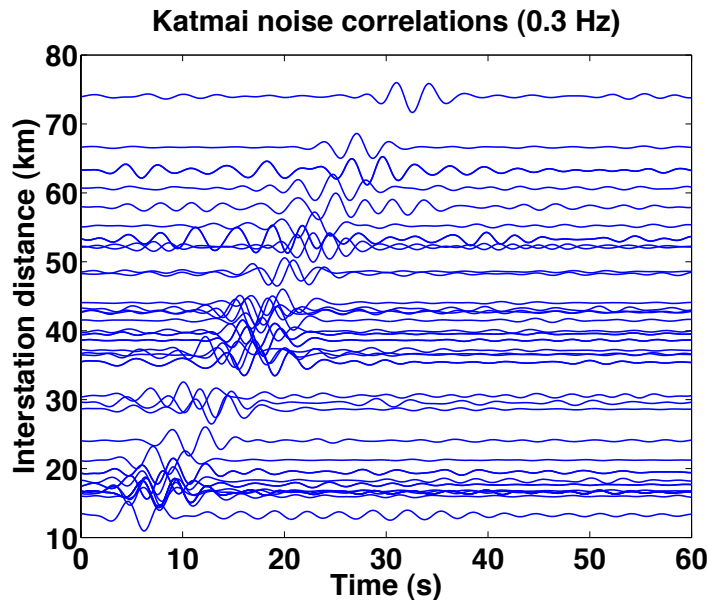


FIG. 2: Correlation Green's functions derived from vertical component recordings of ambient seismic noise within the Katmai network. The correlations are plotted versus interstation distance, highlighting the approximately linear moveout of the Rayleigh wave at 2.5 km/s. A comparison of wavefield simulations to these correlations would provide a strong test of the accuracy of the velocity model used in the simulations [2].

and volcano-scale ambient noise imaging lies in the choice of frequency band - the principles are otherwise identical.

In a recent study in southern California, Ma *et al.* [2] have taken a different approach to using ambient noise. Since the crustal structure in southern California is well known, Ma *et al.* chose to test community velocity models by confronting seismic wavefield simulations with the correlations themselves. For example, the correlations shown in Fig. 2 could be compared to synthetic seismograms using existing velocity models of the Katmai volcanic cluster. This is in contrast to directly imaging the crust using ambient noise. An advantage of such a comparison is that the correlations are oftentimes sensitive to parts of the velocity models poorly sampled by earthquake arrivals.

Given the existing knowledge about the structure of the Cook Inlet basin in Alaska, an approach based on comparing wavefield simulations and noise correlations can demonstrate the shortcomings of the current models of the Cook Inlet basin. In addition, by utilizing recent advances in adjoint tomography based on spectral-element wavefield modeling [6, 7], discrepancies between the wavefield simulations and the noise correlations can lead to improvements in the crustal velocity models of Cook Inlet. For this purpose, a future Earthscope Flexarray deployment in and around the Cook Inlet would provide additional station pairs for ambient noise correlations. In particular, an Earthscope Flexarray would add a considerable number of broadband seismometers, which are necessary to cover the frequency band of interest for basin-scale ambient noise studies, from 0.03-0.25 Hz [5]. We propose 22 additional broadband station sites for a future Earthscope Flexarray deployment in and around the Cook Inlet. The sites are shown in Fig. 1 and are intended to fill gaps in the broadband station coverage from the permanent networks. The addition of 22 stations would bring the total number of broadbands in Cook Inlet, including the permanent networks, to 38. This number of stations is comparable to the broadband array used in the ambient noise study at Hudson Bay [4]. Regarding the sites, it is worth emphasizing that, due to population density and infrastructure, it is comparatively less expensive to deploy instruments in Cook Inlet than other parts of Alaska.

With an expanded broadband network in and around the Cook Inlet, the interstation paths from ambient noise measurements would provide coverage that may be lacking from earthquake-station paths. Furthermore, the ambient noise measurements are independent of unknown earthquake parameters, though source excitation assumptions must be considered. Testing and improving the current Cook Inlet velocity models through comparisons of ambient noise correlations and seismic wavefield simulations should lead to a better understanding of basin structure and associated seismic hazards, in particular basin amplification effects.

-
- [1] P. J. Haeussler, R. L. Bruhn, and T. L. Pratt, *Geological Society of America Bulletin* **112**, 1414 (2000).
 - [2] S. Ma, G. A. Prieto, and G. C. Beroza, *Bulletin of the Seismological Society of America* **98**, 2694 (2008).
 - [3] T. Masterlark, M. Haney, H. Dickinson, T. Fournier, and C. Searcy, *Journal of Geophysical Research* **115**, B02409 (2010).
 - [4] A. Pawlak, D. W. Eaton, I. D. Bastow, J.-M. Kendall, G. Helffrich, J. Wookey, and D. Snyder, *Geophysical Journal International* **184**, 65 (2011).
 - [5] J. A. Calkins, G. A. Abers, G. Ekström, K. C. Creager, and S. Rondenay, *Journal of Geophysical Research*, in press (2011).
 - [6] J. Tromp, Y. Luo, S. Hanasoge, and D. Peter, *Geophysical Journal International* **183**, 791 (2010).
 - [7] D. Peter, D. Komatitsch, Y. Luo, R. Martin, N. L. Goff, E. Casarotti, P. L. Loher, F. Magnoni, Q. Liu, C. Blitz, et al., *Geophysical Journal International*, in press (2011).

Understanding tectonics, mantle structure, volcanism and volatile cycling in North American subduction zones

Erik Hauri

Deep Carbon Observatory-Reservoirs & Fluxes (DCO-REFLEX) and Department of Terrestrial Magnetism, Carnegie Institution of Washington, Washington DC 20015 USA

Introduction

There exist two volatile cycles on the Earth. The surface cycle exhibits rapid movement of water, carbon and other volatiles through multiple organic and inorganic reservoirs via the processes of biological respiration-photosynthesis, combustion of organic matter (by nature and man), weathering and burial of sediment, and exchange between the oceans and atmosphere. The activity of Earth's surface and biosphere has long been the subject of large research initiatives in climate change and global ecology. Yet the surface cycle contains only one-tenth to one-quarter of Earth's budget of volatile elements.

The deep-Earth volatile cycle contains 75-90% of Earth's water and carbon, yet its characteristics are poorly understood when compared with the surface cycle. The deep Earth contains multiple volatile-bearing reservoirs within the lithospheric mantle directly beneath continental and oceanic plates, and carried within the convecting mantle everywhere else. We have solid knowledge of the deep-Earth volatile cycle only in the upper mantle beneath ocean ridges; within subduction zones, and at the great depths of the Earth's transition zone (410-660 km), lower mantle (660-2960 km) much less is known. The sizes, ages, distributions and forms of volatiles in these deep-Earth reservoirs have been only vaguely discerned, and the abundance of volatiles in each reservoir is poorly known, yet it is apparent from surface tectonic activity and volcanism that geofluids can form and be transported to many geophysically active locations within the Earth.

The most significant interfaces between the surficial and deep-Earth volatile cycles are subduction zones, and the main pathways for emergence of geofluids from depth are the subduction megathrust and arc volcanoes. Volatile cycling between the surficial and deep-Earth cycles is completed by returning water-rich organic, inorganic, and biological materials in near-surface sediments and altered oceanic crust to the Earth's interior in subduction zones, where earthquakes great and small testify to the processes of subduction dehydration and deformation. Volcanoes not only deliver important volatile-bearing compounds from the deep-Earth, but also vent volatile-bearing gas species (including greenhouse gases) into the atmosphere on timescales that are important to the surface cycle. Yet the balance of delivery and return fluxes of volatiles between the Earth's surface and interior are so poorly known that we don't even know if the net flux of water is into - or out of - the Earth's interior.

Future focusing of the EarthScope effort in the Alaska-Aleutian arc would provide an important and timely occasion to study the relationships between tectonic forcing, earthquake activity, volcanic unrest, and magmatic volatile transport in an unprecedented and multidisciplinary way (see also white papers by *Plank et al* and *Roman et al*). The Alaska-Aleutian arc is an ideal location to explore these geophysical relationships; the area includes a transition from continental to oceanic crust, a number of active volcanic systems with widely variable pre-eruptive water contents, magma compositions, inferred magmatic storage depths, and active volcanic degassing; large changes in subduction orientation, orthogonal subduction rate and depth to the slab along the strike of the arc; as well as the existence of the full spectrum of tectonic deformation from ETS to great earthquakes. In addition, the Alaska-Aleutian arc is being targeted for comprehensive research efforts over the next decade involving geophysics, geochemistry, and volcanology from GeoPRISMS and the Deep Carbon Observatory.

Never before has so much multidisciplinary effort turned its attention to North American subduction zones as now. The next decade holds great potential for revealing, in unprecedented detail, the geophysical relationships between large-scale tectonics and deformation, mantle structure, mantle volatile content and volcanic activity. Key to this effort will be the simultaneous operation of a number of geophysical and geochemical networks over this intervening period, and the coordination of field work logistics between the organizations involved in this research.

ALASKA LITHOSPHERE AND INNER CORE IMAGING EXPERIMENT (ALICE)

ORIGINALLY PROPOSED TO NSF IN 1989 BY

Alan Levander, Rice University
Douglas Christensen, University of Alaska Fairbanks
Roger Hansen, University of Alaska Fairbanks
Xiaodong Song, now at University of Illinois

Clearly there has been a great deal more learned about Alaska and inner core rotation since we proposed this project in 1989, however a number of the scientific questions are still valid and still debated. The project cost was about \$858K in 1989.

INTRODUCTION

We are proposing a two part passive-source teleseismic investigation of northern Alaska to investigate the structure of the northern Alaskan lithosphere and the rotation and anisotropy of the inner core (Fig. 1). One part of the experiment will employ 12-14 PASSCAL broadband (BB) stations deployed continuously for 2 years NS from Fairbanks to Prudhoe Bay and EW across north-central Alaska to investigate core rotations, structure, and anisotropy and to determine large scale upper mantle structure beneath northern Alaska (Fig.s 1-2). The second part of the experiment will employ 40 additional BB instruments for 5 months to image the details of orogenesis and lithospheric delamination following arc collision with the craton which are preserved in the upper mantle beneath the North Slope, Brooks Range, and terranes to the south. The proposed research has a number of objectives including:

1. Imaging the upper mantle and lower crust of northern Alaska to examine subduction of the lower crust and delamination of the lithosphere in the Jurassic-Recent Brooks Range fold and thrust belt beneath the North American craton of the North Slope. The subduction event was imaged by the 1990 Brooks Range active source experiment, but could be traced only to 65km depth, and approximately 60km into the mantle north of the front of the Brooks Range due to the shot-receiver configuration (Fig. 3). This 5-6km thick mafic lower crustal layer is likely metamorphosed to eclogite in the lower-crust/upper mantle and therefore will make an excellent target for receiver function imaging, as was shown recently in the Lithoprobe SNORCLE profile (Fig. 4). A receiver function image made from a dense array of instruments will map mantle structures associated with the lower crustal subduction/delamination event (Fig 4., Bostock, 1998, see also Dueker and Sheehan, 1997).
2. Imaging other lithospheric mantle structures beneath the island arc terranes and minor collapse structures associated with the Brookean orogeny as well as collisional arc and the strike-slip accreted terranes lying between the Brooks Range and Tintina Fault in northern Alaska.
3. Imaging the transition zone beneath a modern orogenic belt, the Brooks Range, and the minor collapse and major strike-slip structures to the south and the North American craton to the north, and determining P and S wave velocity structure of northern. We are particularly interested in S-wave anisotropy in the Brooks Range, which has been determined to be very large, both from a pilot teleseismic BB experiment (Christensen, 1991), and from rock samples analyzed as part of the active source experiments (N.I. Christensen, 1995, unpublished report).
4. Measurements to resolve critical issues concerning the rotation and anisotropy of the inner core. Recent seismological observations on the anisotropy and rotation of the inner core and numerical simulations of the geodynamo have advanced considerably our knowledge of the structure and the

dynamics at the center of the Earth. Further advances are limited by the lack of data at critical locations and orientations, such as a dense array at high latitudes for north-south waves from the Earth's core. Seismograms recorded at stations in Alaska from earthquakes in the South Sandwich Islands (SSI) have played a critical role in inferring the inner core anisotropy and the inner core rotation. However, because almost all the existing stations are distributed in southern Alaska, the critical part of the inner core sampled by previous SSI earthquakes, as the inner core rotates eastwards, can only be imaged by deploying stations in northern Alaska. Recent observations of a possible transition zone inside the inner core need to be further imaged with data sampling different depths of the inner core with stations in the interior of Alaska. Dynamo models that produce similar magnetic fields at the Earth's surface show very different behaviors of the inner core motion. Just as astronomers set up special telescopes to see distant stars, we will set up a special experiment to "see" the distant inner core of our planet.

TECTONIC OVERVIEW OF ALASKA

Alaska is tectonically unique in that over a distance of ~1250km one crosses from an active convergent margin where the Pacific plate is subducting beneath southern Alaska to a rifted passive margin forming the northern margin of the North American craton (Figs 1-2). In addition to 1) the subduction related accretionary terranes and continental arc in the south, Alaska consists of 2) a succession of strike-slip accreted terranes between the Denali fault in south central Alaska and the Tintina-Kobuk-Kaltag fault system extending from north-central Alaska to the southern edge of the Brooks Range, 3) a modern north-vergent fold and thrust belt, the Brooks Range, and its foreland basin, which rests on 4) the northernmost element of the North American craton. The northern edge of the North American craton at the Arctic coast is 5) an early Cretaceous passive margin. An ongoing passive source seismic experiment operated by the University of Alaska at Fairbanks (BEAAR; Christensen & Hansen) in south central Alaska is currently examining structure under the Alaska Range and subduction complex. This proposal is concerned with northern Alaska from Fairbanks to Prudhoe Bay, essentially dovetailing with the BEAAR experiment and will complete a study from the southern Alaskan subduction zone to the Arctic passive margin.

Grand's (1994) teleseismic S-wave model of North America shows that northern Alaska has moderately high (i.e. cratonic) mantle S velocities extending to depths > 250km, although Alaska is on the edge of the study area. Zhao et al. (1995) have produced high resolution P-velocity tomography images of the southern Alaska subduction zone to 200km depth from the Alaska seismic network concentrated in southern Alaska. At depths > 65km the image extends no further north than Fairbanks, however. One part of this proposal is to investigate the Alaskan lithosphere north of Fairbanks, including the Brooks Range and flanking terranes.

The Brooks Range, the northernmost element of the North American Cordillera, is a Jurassic-Recent aged, east-west trending, north-vergent fold and thrust belt (Fig. 1). An overview of the development of the fold and thrust belt is given by Blythe et al. (1996) which we paraphrase here. In the Jurassic, the southern edge of the Alaskan North American craton was a passive continental margin. In the Late Jurassic to Early Cretaceous this passive margin was shortened by collision with an island arc, forming the Brooks Range and its foreland basin on the North Slope. Remnants of this island arc, which were accreted to the southern Alaska margin by 130-100 Ma, are now found in the Yukon-Koyukuk Basin on the southern flank of the Brooks Range. Simultaneously, the Canada basin opened, forming the northern passive margin now found along the Arctic Ocean. The southern part of the Brooks Range experienced variable amounts of extension in the period 130-90 Ma (Gottschalk and Oldow, 1988; Miller and Hudson, 1991, Till et al., 1993), followed by significant shortening again in the Tertiary between 60 Ma and 25 Ma. The latter is likely the result of low-angle subduction of the Kula plate along the north-dipping southern Alaska subduction zone.

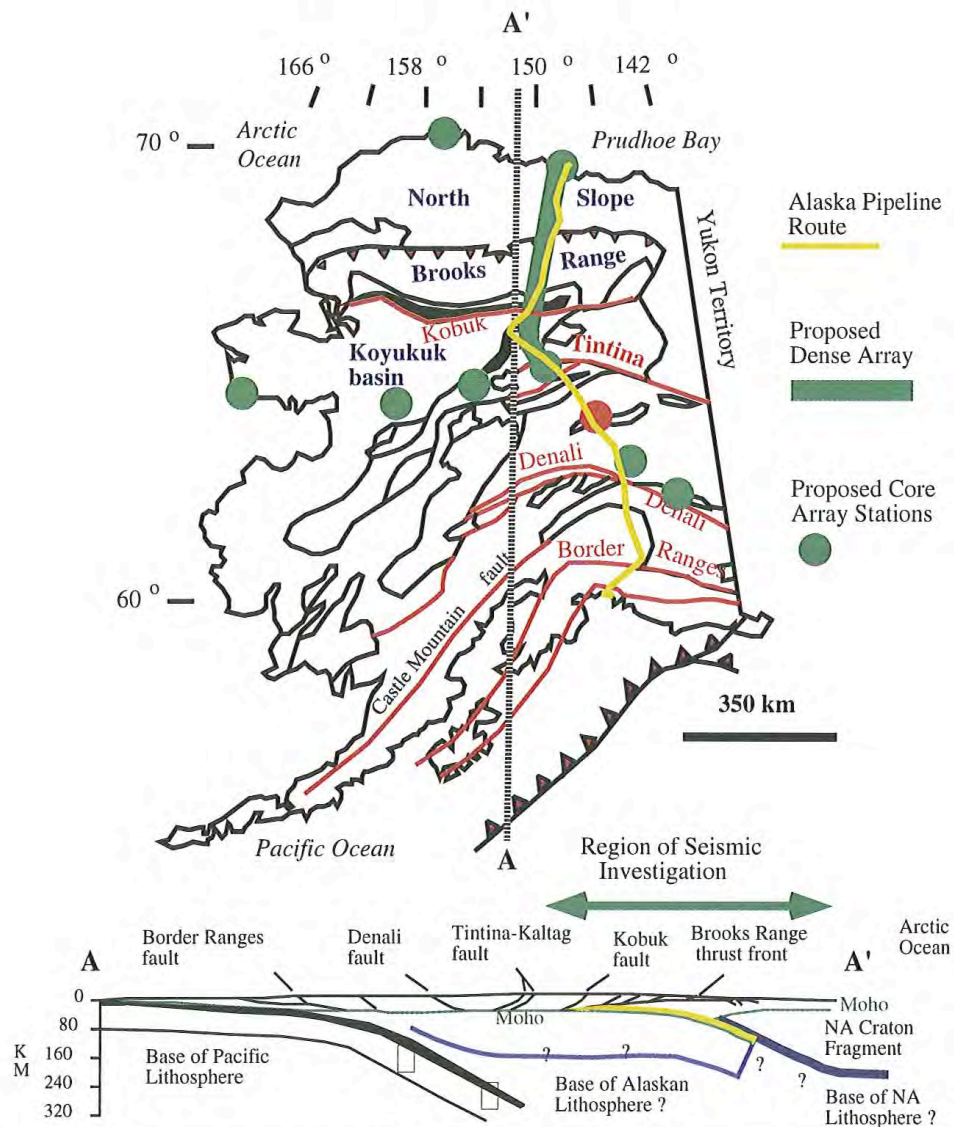


Fig. 1 Generalized geologic map of Alaska (Jones et al., 1981) and cross-section (modified after Wissinger, 1995; Oldow et al., 1989). The proposed dense BB array is shown as a solid green line. Individual stations for the core array not nested within the dense array are shown as green circles.

Principal faults are in red. The oceanic subduction zone in southern Alaska and the frontal thrust of the Brooks Range in northern Alaska are shown with red teeth. The Brooks Range frontal thrust overlies a zone of **north vergent** intracontinental subduction, shown in the cross section. The yellow layer in the cross-section denotes the lower crustal layer subducting against the craton in northernmost Alaska. The deeper upper mantle structure north of the Tintina Fault is virtually unknown. The area south of Fairbanks and the Denali fault is being investigated by the BEAAR experiment.

The Brooks Range is largely deformed non- to highly-metamorphosed passive margin sediments of mid-Paleozoic age that have been displaced along a system of thrust faults extending to lower crustal depths and overthrust by ophiolitic rocks during the island arc collision (Mull, 1982). The assemblages of the Brooks Range are subdivided into major thrust bounded terranes based on similarities in structure,

stratigraphy, and/or metamorphism (Figs 1-3). South of the Brooks Range are the Yukon-Koyukuk basin, containing 5-8 km of mid-Cretaceous-Recent sediments (Box and Patton, 1985) which may be a late Mesozoic collapse structure, and the Ruby terrane, a linear uplift trending diagonally across central Alaska composed of Paleozoic continental and island arc rocks and Cretaceous plutons.

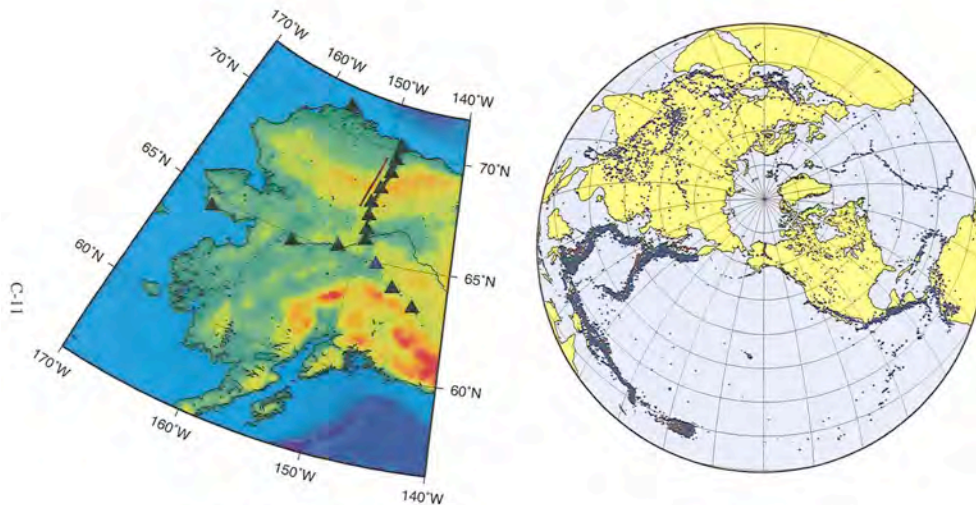
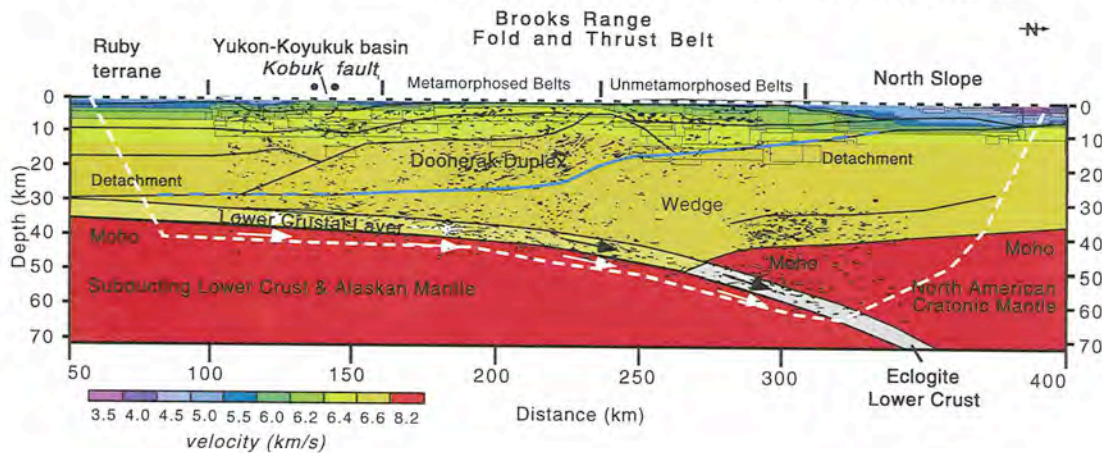


Figure 2. Left: Alaskan topography and proposed seismic arrays. Core stations are large triangles. station COL is shown in blue; the dense array are small triangles. The 1990 active source experiment is shown as a red line. Right: Source regions from 30 to 90 deg from the center of the dense array. Hypocenter depths are color-coded: blue - above 200 km, green - between 200 and 400 km, red - deeper than 400 km. The dense array is well positioned for deep events including the Fiji-Tonga trench.

The internal structure of the Brooks Range was investigated in the 1988 and 1990 active source Brooks Range experiments by the USGS and Rice University (Levander et al., 1994; Fuis et al., 1995, 1997; Wissinger et al., 1997, 1998). The active source experiment extended from the Ruby arc terrane in the south across the folded belt, and halfway across the North Slope (Figs 1&3). Coincident with the active source experiments Christensen et al. (1991) deployed 4 BB stations to investigate crustal structure with receiver function inversion, and to examine S-wave splitting. The Brooks Range is an excellent tectonic target for seismic investigation because it is a Mesozoic-Recent Cordilleran type folded belt, only the southern-most part of which has been affected by Cenozoic extension. It is logistically accessible along the Trans-Alaska Pipeline Haul Road, along which an extensive cultural infrastructure exists. Lastly, seismic noise levels are low, and signal propagation proved to be excellent.

The active source experiment determined the internal velocity and reflectivity structure of the Brooks Range, which included a seismic reflection image of crustal duplexing, in which half of the crust has been simultaneously involved in lateral transport and thickening (Fig. 3: see also Cook, 1997). The receiver function determinations of S-wave crustal velocity are in excellent agreement with the P-velocity determined from the active source study. The BB study also identified large S-wave splitting (0.4 to 0.87s) with rapid variation in fast direction over short distances across the range, from 64 deg. in the south to 170 deg. in the north.

Fig. 3 Velocity model of the Brooks Range from 1990 active source experiment with migrated reflectivity patterns and major layer boundaries shown. (modified from Wissinger et al., 1997). Reflection geometry indicates lower crust/mantle subduction beneath the North Slope. Velocity of the subducted lower crust is unconstrained. White dashed line indicates the area illuminated by refractions from the active source experiment.



One conclusion drawn from the reflectivity structure of the Brooks Range is that a 5 km thick reflective zone just above the Moho acted as a detachment zone beneath much of the range. At very least, the rocks above the top of this zone are detached from those below. Moreover, the active source experiment produced a very clear view of lower crustal subduction into the upper mantle and upper mantle deformation beneath the North Slope at the northern edge of Range (Fig. 3; Wissinger et al. 1997; Fuis et al., 1997). Unfortunately no BB station was deployed far enough north to observe this. The subducting lower crust is likely eclogitized while entering the mantle or shortly thereafter and has mantle-like seismic velocity. A ~5 km thick section of crust is subducting into the mantle and preserving a reflectivity structure. This type of subduction has been termed delamination, intracontinental subduction, and Type A subduction (as opposed to normal subduction, oceanic plate subduction, and Type B subduction) by various researchers. This is a semantic point.

Estimates of shortening in the Brooks Range based on the seismic reflection data vary from 250 to 600 km based on restoration assumptions (Fuis et al., 1995, Wissinger et al., 1998). An equivalent level of shortening must have occurred in the lower crust, meaning that 250 to 600 km of lower crust has returned to the mantle. The balanced cross-section reconstructions (Wissinger, 1998) imply that $\sim\frac{1}{2}$ of the initial passive margin now forms the mountain belt, $\sim\frac{1}{4}$ has been subducted, and $\sim\frac{1}{4}$ has been eroded and redistributed in the surrounding basins (Levander, unpublished). Some shortening models of the Laramide contraction in the Rockies predict large mass transfer from the mountain belt to the crust of the Great Plains (e.g. Bird 1987) to explain the Plains excess crustal thickness (e.g. Sheehan et al., 1997). In the Brooks Range the active source data show that this type of crustal mass transfer has not occurred, as 1) rocks immediately above the Moho are clearly involved in surface related structures, 2) crustal mass is transferred to the mantle at the range front (although a small midcrustal region at the front of the range likely represents middle crust mass flow, identified as WEDGE in Fig 3.), and 3) crustal thickness decreases from ~50 km beneath the range to <40 beneath the North Slope, (i.e. to cratonic values, Christianson and Mooney, 1995), indicating that large volumes of mass have not been laterally transferred from the Brooks Range to the North Slope crust.

CONTINENTAL SUBDUCTION AND DELAMINATION

We are proposing to investigate the structure of the lithosphere beneath the North Slope and Brooks Range to examine the continental subduction and delamination process: We wish to determine the fate of the lower crust subducted against the edge of a craton. Delamination of lithospheric mantle, with or without lower crust has been proposed for orogenic belts worldwide as an important process in the

orogenic cycle (e.g. Nelson, 1991). For example Kay and Kay (1991) have suggested delamination is occurring beneath the Altiplano-Andes and the Alps based on a variety of data. Owens and Zandt (1997) have seismic evidence that delamination is occurring beneath the Tibetan Plateau. Sever et al. (1994) have proposed delamination beneath northern Morocco based on seismicity and other data. Active source seismic images suggesting or showing delamination processes are available not only from the Brooks Range, but also the Alps (ETH Working Group, 1991), the Pyrennes (Choukroune,1989), and spectacularly, beneath the Wopmay orogen adjacent to the Slave Craton in Canada (Fig. 4; Bostock, 1998). The SNORCLE active source data are in excellent agreement with Bostock's receiver functions from the Yellowknife array (Fig. 4). The details of this delamination process are unclear beneath the Andes, Alps, Pyrennes and Tibetan Plateau. The SNORCLE data show the subducted lower crust (which in this case may have been oceanic, not continental) to a depth of 100 km over more than 200 km distance. Other upper mantle reflectors can be traced over a distance of 500 km. The receiver functions show bright events coincident with the reflection data at 80-100km depth and a possible steeply dipping event at 180-220km depth (Fig 4).

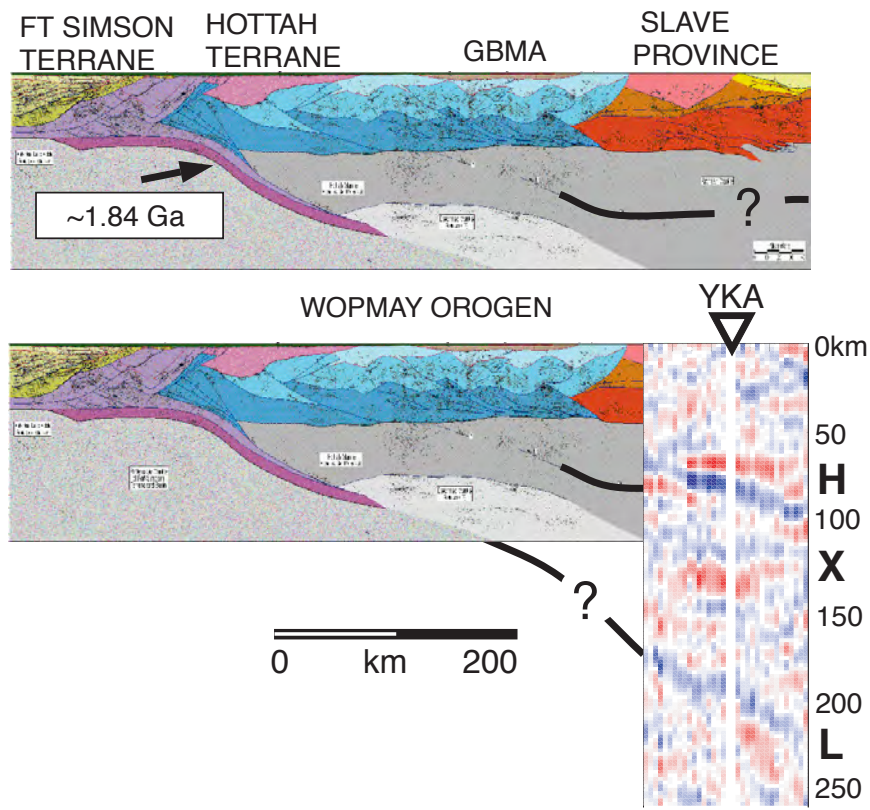


Fig 4: Reflection data and receiver function section from the Yellowknife Array (YKA) from the Slave NORthern Canada Lithosphere Experiment (SNORCLE). The receiver function event H is in correspondence with a zone of high reflectivity at 80 to 100km depth. Event L may coincide with the subducted crust (purple) extending from the Moho at 50km to 100km depth in the reflection section. The section shows lithospheric mantle shortening and thickening against the Slave craton tectosphere. Mantle shortening is as important as crustal shortening in the development of orogenic belts; note the interpreted crustal thrust structures above 50km depth. Figure from Bostock (1998); reflection data from Cook (1998). The continental subduction event beneath the Brooks Range likely has equally intriguing details which should be imaged by the proposed dense BB receiver function section.

The question arises as to whether these events represent convective overturn of the lithospheric mantle which also happens to involve the crust (e.g., Houseman et al., 1981), or whether they are part of advective thickening of the peripheries of cratonic tectospheric roots (Jordan, 1978, 1988). The details of either of these processes are poorly understood at present. The Brooks Range-North Slope offers an excellent study area, and the available active source data show large scale crust-mantle interaction, while available passive source data from YKA as well as data from ocean-continent subduction zones (e.g., Nabelek et al., 1993) indicates a high likelihood of imaging the structures with teleseismic data.

PROPOSED RESEARCH: TINTINA-BROOKS RANGE-NORTH SLOPE DENSE ARRAY

We are proposing to deploy a dense (~12.5 km increment) array of BB instruments across the North Slope and Brooks Range from Prudhoe Bay to the Tintina Fault near the Yukon River to investigate the upper mantle beneath the orogenic belt and North Slope, particularly to examine the continental subduction structure. We will also investigate the whole orogenic belt mantle structure and that of the arc/collapse and strike slip terranes south of the range, as well as anisotropy within and outside of the range. Details of the deployments are described in a later section. The dense station spacing will permit a reflection style receiver function image craton (Dueker and Sheehan, 1997) for investigating the lower crustal layer where it subducted and collided with the tectospheric mantle of the northern Alaska. It is likely that other significant mantle structures exist beneath this orogenic belt where 250-600km of shortening occurred, beneath the island arc which collided with the Brooks Range, and beneath the collapse and strike slip structures south of the range. Tomographic velocity models, shear wave splits, and receiver functions will be used to determine upper mantle structure. We will also be able to look for systematic variations in transition zone structures crossing from the accreted terranes of north central Alaska which are the result of subduction and strike-slip to the orogenic belt, the result of arc collision and shortening, and then from the orogenic belt to the northern craton.

The PDE 's for the last 30 years show an average of 60 events/month greater than $m_b > 5.0$ in the distance range $30^\circ < \Delta < 90^\circ$ from the center of the array (Fig. 2). In five months the dense array will record ~300 earthquakes. The PDEs suggest we should record 17 earthquakes with $250\text{km} < h < 400\text{km}$ and 13 with depths greater than 400 km in this distance range. Northern Alaska has extremely low noise conditions, making it likely that we will be able to use an unusually high percentage of the data we acquire for tomography and receiver function studies. The array is well aligned with the Tonga-Fiji source region, but is oblique to normal to other Pacific or South American sources. Logistically, however, this is the only feasible deployment plan without spending millions of dollars on helicopters, as northern Alaska has only one road.

INTRODUCTION AND BACKGROUND TO THE PROPOSED INNER CORE STUDIES

The dynamo action in the metallic fluid outer core, which generates and maintains the Earth's magnetic field, was expected to drive the conducting inner core to rotate at a rate different from the rest of the Earth through electromagnetic coupling (e.g. Gubbins, 1981; Glatzmaier and Roberts, 1995). Observational evidence for a differential rotation of the inner core have recently been reported from seismic waves that penetrate the inner core (Song and Richards, 1996; Su et al, 1996; Creager, 1997; Ovtchinnikov et al., 1998; Li et al., 1998). The inner core rotation was inferred from observations of temporal variations of inner core arrival times caused by the shifts of asymmetric structure (e.g. tilt of the symmetry axis or lateral variation) of the inner core anisotropy, first proposed by Morelli and Dziewonski (1986) and Wouldhouse et al. (1986) and well-established in recent years by the work of Creager, Tromp, Song and Helmberger, Shearer, and many others. Seismograms recorded at stations in Alaska from earthquakes in the South Sandwich Islands (SSI) have played a critical role in inferring the inner core anisotropy (Creager, 1992) and the inner core rotation (Song and Richards, 1996; Song, 1999, see below). However, because almost all the existing stations are distributed in southern Alaska, the critical part of the

inner core which was sampled by previous SSI earthquakes, as the inner core rotates eastwards, can only be imaged by stations in northern Alaska as proposed here. In addition, stations in northern Alaska can provide vital depth resolution of the core anisotropy for confirming and resolving our recent observation of an inner core transition, which separates an isotropic upper inner core and an anisotropic lower inner core (Song and Helmberger, 1998; also see below).

OBSERVATIONS OF INNER CORE ROTATION FROM STATIONS IN ALASKA

Song and Richards (1996) examined differential travel times between PKP(BC) and PKP(DF) for paths from earthquakes at almost the same location but decades apart to the same monitoring station. The use of differential travel times reduces biases from mantle heterogeneity and earthquake location errors. They found that the BC-DF differential times along certain pathways, including a pathway from earthquakes in South Sandwich Islands (SSI) to station at College, Alaska (COL), have changed systematically with time. The temporal changes were interpreted as evidence for a differential inner-core rotation, which moves the axis of the inner core anisotropy: The rotation rate was estimated to be about $1^\circ/\text{year}$. Further estimates of the rotation rate vary by orders of magnitude from $3^\circ/\text{year}$ by Su et al. (1996) to $0.2\text{-}0.3^\circ/\text{year}$ or even as low as $0.05^\circ/\text{year}$ by Creager (1997). An attempt by Souriau (1998) to detect the inner core rotation was unsuccessful but she could not rule out a rotation of less than $1^\circ/\text{year}$.

To confirm and constrain the inner core rotation, Song (1999) recently examined both historical and modern seismograms from SSI events recorded at COL and Alaska Seismic Network stations (ASN). Original paper records of SSI earthquakes at COL between 1951 and 1966 were found at the U.S.G.S. office in Golden, Colorado, extending the previous measurements at COL by Song and Richards (1996) back an additional 15 years. The Geophysical Institute of the University of Alaska at Fairbanks (UAFGI) has been operating the Alaskan Seismic Network (ASN) with over 100 stations since the late 1960s. Most ASN stations are short-period vertical component instruments peaked at 1 Hz. Virtually complete archives of seismograms are still available at UAFGI, but most of the archives are in microchip form (Develocorders), precluding recovery of waveforms. Paper seismograms (Helicorders) are available for a limited number of stations. Digital recording of analog signals started around 1989.

Fig. 5 shows BC-DF differential travel-time residuals as a function of earthquake occurrence time at COL and three ASN stations Yukon (FYU), McKinley (MCK), and Sheep Creek Mountain (SCM) (which are 140 to 540 km apart from each other and from COL). All the events have been relocated in the Joint-Hypocenter Determination method by Dewey (1971). We observe a clear time-dependence of the BC-DF times at all the stations (Fig. 5). The new measurements at COL for earthquakes in the 1950s and early 1960s are consistent with the temporal change observed previously (Song and Richards, 1996). The trend of gradual increase in the BC-DF times at COL is striking; over the past 45-year-period (1951 through 1995), the BC-DF times have increased by 0.54 s. The null hypothesis that there is no correlation between the residuals and the event times is rejected at a significance level of 0.05% for FYU, 0.02% for MCK, about one out of a million for SCM, and less than one out of a billion for COL. Even though the linear correlation coefficient for the COL observations is smaller than those for FYU, SCM, the larger number of samples greatly reduces the significance level (i.e. increases the confidence level) at which the null hypothesis is rejected.

The inference of the rotation rate from the observed travel-time variations depends on the local lateral velocity changes in the part of the inner core sampled by the paths. We have collected all the digital ASN records from $m_b > 5.19$ SSI events in 1991-1998. We obtained 543 high-quality BC-DF measurements from the digital records in 1990s, which are shown in Fig. 6A together the 68 measurements at COL, FYU, MCK, and SCM from SSI earthquakes before 1990. This large data set confirms significant changes in BC-DF residuals along ray bottoming points in the inner core from east to west (Fig. 6B) suggested previously by Creager (1997).

Imaging the local lateral velocity changes of the inner core, however, can be severely biased by mantle heterogeneity, causing uncertainties in estimating the rotation. Realizing that the mantle biases do not change as the inner core rotates, Song (1999) proposed a joint inversion scheme to separated time-

dependent inner core structure from mantle biases. Our inversion results suggest that the robust temporal changes of the differential BC-DF travel times at ASN and COL stations can be interpreted by a differential inner core rotation that shifts the lateral velocity changes present at this part of the inner core and, possibly, the orientation of the anisotropy axis (if it is tilted from the inner core rotation axis). The lateral velocity gradient is found to be robust and very significant, but some 50% of the lateral changes in original residuals (Fig. 6A) can be explained by mantle heterogeneities.

Our estimates of the rotation rate from inversions that include mantle corrections fall within a tight range from $0.31^\circ/\text{year}$ to $1.10^\circ/\text{year}$, even when a tilt of up to 10° is considered; the average is $0.81 \pm 0.18^\circ/\text{year}$ when no tilt of the anisotropy axis is assumed and about half of that when a 10° tilt is assumed. The average of these two end member models is $0.60 \pm 0.26^\circ/\text{year}$. The null hypothesis that the inner core is not rotating or is rotating westwards can be rejected at confidence level of more than 99.99% in our joint-inversion with the large ASN dataset. Further constraint on the inner core lateral variation and the rotation is hindered by the fact that there is few samples of the part of the inner core [70° - 60° W in Fig. 6] which was sampled by the historical data.

AN INNER CORE TRANSITION ZONE FROM BROADBAND OBSERVATIONS IN ALASKA AND CANADA

Song and Helmberger (1998) observed evidence for a possible inner core transition zone. An important line of evidence comes from compelling differences between BB waveforms along NS paths from SSI events to Alaska and Canada and those from EW paths (Fig. 7). The waveforms of the DF phases from the EW paths are similar to the corresponding BC waveforms with the exception of a slight broadening and less high frequency content in the DF waveforms due to inner core attenuation (e.g., Doornbos, 1974). The difference in time of the DF versus the BC arrivals is well predicted by the reference model PREM2 (Song and Helmberger, 1995).

In contrast, the DF phases from the NS paths arrive earlier than predicted by the reference model, as attributed to inner core anisotropy, and have much broader waveforms than the corresponding BC or AB phases. Note the sharp contrast in DF waveforms and BC-DF differential times between the EW path from Event 11 in the South Sandwich Islands (SSI) to station INCN in Korea and the NS paths from the same event to KDAK, COLA in Alaska and INK in Canada.

The anomalously broad waveforms in the Canadian and Alaska records can be explained by a triplication caused by a sharp velocity jump within the inner core encountered by the NS paths if the inner core is divided into an isotropic upper part and an anisotropic lower part. The model with a P velocity jump of 4.3% at 250 km below the ICB reproduces reasonably well the broad DF waveforms of the NS paths. Synthetics generated for our smooth reference model, PREM2, fit the waveforms of the EW paths rather well; the isotropic-anisotropic transition becomes much less pronounced for EW traveling waves.

Because only two BB stations (COL, KDAK) in Alaska are available at the critical triplication distances, we were forced to use different earthquakes to construct a record section to see how the triplication moves with distance.

PROPOSED INNER CORE STUDIES

The major goals on the inner core studies of the integrated PASSCAL experiment are 1). To obtain high resolution of lateral variation of inner core anisotropy beneath the Caribbean Sea and northern Venezuela sampled by historical SSI events to Alaskan stations for further determination of inner core rotation; and 2). To provide NS samples of the inner core at distances around 152° (SSI-COL) \pm a few degrees from a same seismic source for resolving the structure and nature of the observed inner core transition. These samples can be obtained only by deploying stations in the interior of northern Alaska. Our targeted SSI source region is seismically the most active region as well as being the only subduction zone in high latitudes in the southern hemisphere.

From 1964 through 1997, 726 SSI events have been reported (by PDE) with m_b 5.2 or larger, with an average of 21.4 ± 15.0 (2 sigma) per year. In each every year during the 33-year period, 10 or more m_b 5.2 events occurred, with the exception of 1996 (only 5 events). Thus, in the 24-month planned period of the experiment, we can reasonably expect more than 13 SSI events (the lower limit of 2 sigma error) with m_b 5.2 or larger to occur.

(1) Inner Core Rotation: Of all the NS paths examined for the inner core rotation by us and others, the pathways from SSI events to COL, FYU, MCK, SCM provide the most robust observations with COL having the longest period of recording and the largest observed temporal changes in BC-DF times. On the other hand, despite our thorough search of ASN data, we found few samples of the part of the inner core (east of 70°W in Fig. 6) that was sampled by the historical SSI events to COL, FYU, MCK, SCM because of the lack of stations in northern Alaska at appropriate distances. The three outliers at 65° - 60°W are from a station at Katktovic (which operated for only two years) and a station at Barrow (which is not at a good distance from the active areas in SSI) along the north coast of Alaska. Sampling of this part of the inner core is critical in confirming the lateral velocity gradient imaged from the ASN stations sampling west of 70°W for constraining the rotation rate.

To obtain such samples, it does not help for us to wait because this part of the inner core will rotate away and can only be seen from the Arctic Ocean as the inner core continues to rotate eastward. Using seismograms from the same source also allows us to reduce biases from source mislocation on the estimate of the lateral variation.

(2) Transitional UIC/LIC Structure: The resolution of the UIC/LIC structure is limited by insufficient data at key locations. For example, determining how the BB waveforms (Fig. 7) change at distances outside the narrow 2° distance range now available will greatly help in determining the depth and the velocity jump at the boundary. Records from the same source are also essential in separating source time functions from wave propagation. The stations at Tanana, and Galena, Alaska, are chosen for this purpose. The additions of these stations to existing stations in Canada (120° - 147°) and Eastern Siberia (160° - 178°) (used previously by Vinnik et al., 1994) also provide a continuous distance coverage of PKP waves along NS paths from SSI events, which is extremely valuable for constraining the depth-dependence of the inner core anisotropy and attenuation.

EXPERIMENT PLAN

The array deployment plan is shown in Figs 1 and 2. All of the core array stations are accessible by road or by commercial air service. The core array will be deployed in the first summer of the experiment, during which time the sites for the dense northern array will be prepared. All of the core array sites will be located in villages or at year round maintenance centers operated by the Alaska Department of Transportation and service centers operated by the Aleyska Pipeline Company along the Haul Road. These Haul Road centers and the villages have power and telecommunications. The centers along the Haul road are located at about the desire station interval ($\sim 100\text{km}$) for the core array, and are large enough that quiet recording sites with power can be secured.

The dense array will be deployed in late April of the second year and operated until the end of September. The dense array stations will be powered by car batteries and solar panels (much of the array is at or above the Arctic Circle and will have 24 hour daylight through much of the deployment). Six to seven of the core array stations will be within the dense array giving the dense array a length of $\sim 600\text{km}$. The core array will be removed and the dense array sites cleaned up in the third summer.

During the first summer while preparing the dense array sites, personnel from Rice and LDEO will operate the core array, providing maintenance experience for the Rice/LDEO personnel before the dense array deployment. Personnel from Rice and LDEO will also operate the core array the second summer. The core array will be maintained by experienced UAF personnel based in Fairbanks for the 16 winter

months of the 24 month deployment. The dense array and most of the core array will be serviced from Prudhoe Bay, the Toolik Lake Biological Research Station in the northern Brooks Range, and the Coldfoot Services Center (a truckstop and tourist enterprise) in the southern range in the summer. Levander has worked from these facilities in 1988 and 1990.

We make a number of notes regarding the field acquisition. First, it is impractical to service the dense array in the winter in northern Alaska. It would be better to deploy the dense array for 2 summers, but this would increase the budget by >\$100,000 due to shipping and personnel costs. Second, if the PASSCAL broadband array is available for the experiment it would be an excellent instrument to use on the North Slope and in the northern Brooks Range. The area is entirely above treeline and offers commanding heights accessible by road. In the 1988 active experiment we used a low power FM SGR system and could broadcast for 35km in the Brooks Range. (The system was designed to operate over ~10km).

CONCLUSIONS

These two experiments are coupled and complement one another. The core array will provide better regional compressional and shear wave velocity models for northern Alaska than are currently available, which will in turn help place the dense array measurements in tectonic context. Given that we will likely record 5 SSI earthquakes on the dense array, help to improve time measurements with stacking techniques. Normal S/N improvement through stacking would be ~7, although structural irregularity does not stack out according to the random noise model. Nonetheless we should be able to substantially improve timing and remove ambiguity in core measurements arising from local structure. The mantle structure imaged using mantle phases can also be compared with mantle biases obtained from joint inversions for the time-dependent inner core structure using core phases.

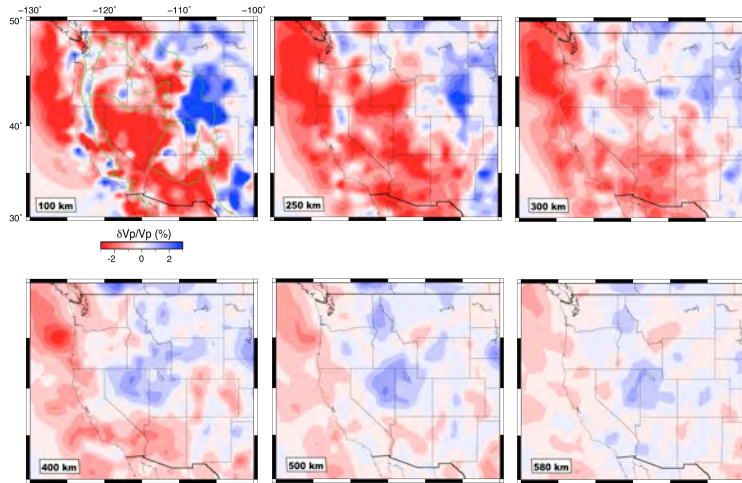
We are examining two fundamentally different parts of the Earth using two coupled arrays: The proposed research will 1) examine crust-mantle processes of orogenesis and continental crustal subduction, and lithospheric delamination in a region already well explored with crustal active source data, and 2) examine fundamental aspects of the Earth's core rotation and inner core-outer core structure and dynamics. Although moderately expensive this project will address a range of Earth science questions which vary from crustal recycling and therefore the composition of the Earth's crust, to the rotation of the inner core and therefore the workings of the geodynamo.

Segmentation of the Farallon slab

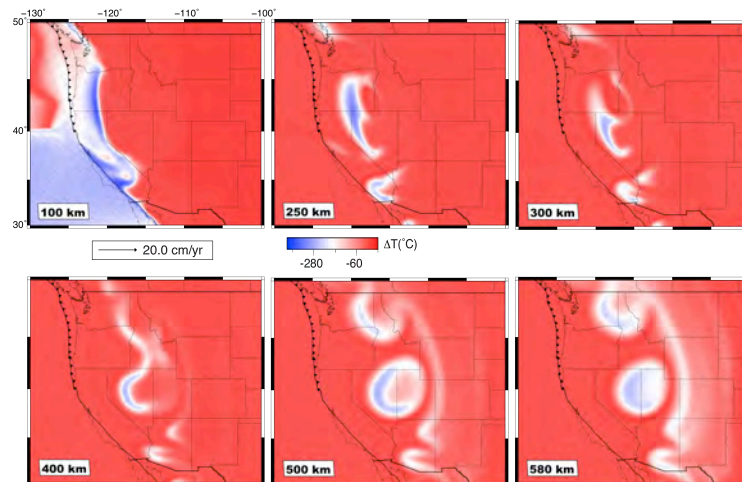
Lijun Liu & Dave Stegman

IGPP, Scripps Institution of Oceanography, University of California, San Diego, CA, 92093

We investigate subduction of the Farallon-Juan de Fuca plate during the past 40 Ma using 3-D numerical models. By assimilating plate motion history, paleo-age of sea floor, and paleo-geography of plate boundaries, we attempt to reproduce the recently observed complex mantle structure beneath western U.S. as reported by seismic tomographic models using EarthScope data (Fig. 1, model by Sigloch, 2011). Using forward models, we show that the highly segmented western U.S. upper mantle structure is a result of the time history of Farallon-Juan de Fuca



subduction, subject to the opening of a slab window and Basin & Range (B&R) extension since 30 Ma. The imaged fast seismic anomalies located between 300-600 km depth bear little resemblance with the shallower portion (above 300 km), as suggested by most recent tomography inversions. We find that the tilted ‘cylinder’-shaped fast anomalies presently beneath Nevada and Utah are subducted slabs since 15 Ma, while the linear slab imaged beneath the Cascades is younger than 5 Ma in general (Fig. 2). The distinct morphology between these two parts of the subduction system indicates the strong influence of toroidal flow induced by the sinking slab, originating from the migrating JF-PA-NA triple-junction and the development of the B&R extension. Details of the slab structures at depth are sensitive to both the radial viscosity profile in the mantle and lateral viscosity contrast of the modeled slabs. Our subduction model for western U.S. also appears to be consistent with the evolution of several structural geologic features within the B&R province.



Stalling and Storage of Magma in the Crust

Terry Plank (*LDEO*), Mindy Zimmer (*LANL*), Erik Hauri (*CIW*), Paul Wallace (*Oregon*), Brad Singer (*Wisconsin*), Brian Jicha (*Wisconsin*), Jess Larsen (*AVO*), Chris Nye (*AVO*), Katie Kelley (*URI*), Jeff Freymueller (*Alaska*), Pete Stelling (*W.Washington*), Gene Yogodzinski (*S.Carolina*) Diana Roman (*CIW*).

In the past decade, the first baseline data have been obtained on the pre-eruptive water contents for several arc volcanoes worldwide. Combined with CO₂, water concentrations at vapor saturation potentially constrain the maximum depth of magma stalling prior to eruption. At the same time, GPS, InSAR and seismic arrays provide near real-time information on magma storage and movement in the crust. These independent data streams thus intersect on the important science questions of where magmas stall in the crust, and how much magma remains versus erupts. These questions are central to the EarthScope and GeoPrisms science themes that bear on the structure and growth of continental crust, the cycling of fluids through subduction zones, and the drivers for explosive eruptions.

One curious observation is that prior to eruption, mafic arc magmas contain a maximum of ~ 4 wt% H₂O on average at each arc worldwide. Within each arc, the variation is generally from 2 to 6 wt% H₂O, with few exceptions. The similar averages at different arcs is unexpected given the order of magnitude variations that occur in other geochemical tracers from the subducting slab. H₂O is clearly different from other tracers, however, being both a major driver of melting in the mantle and a major control on the buoyancy and viscosity of magma in the crust. The range of H₂O contents observed is consistent with magmas reaching H₂O-saturation in the upper crust (< 15 km depth). This is also consistent with the depths of magma storage beneath active volcanoes, as inferred geodetically or imaged seismically. Do magmas stall in the upper crust because of external drivers (stress state, crustal rheological structure) or because of internal magmatic parameters (magma buoyancy and viscosity)?

The Alaska-Aleutian arc is a prime location to explore magma stalling, because active volcanoes vary more than elsewhere in the world in pre-eruptive H₂O contents and inferred magma storage depths. For example, Shishaldin volcano taps magma with among the lowest H₂O contents globally (~ 2 wt%) and records low pressure crystal fractionation (*Zimmer et al., J.Pet., 2010*), both of which are consistent with a shallow magma system (< 1 km bsl). At the other extreme, Augustine volcano is fed by a mafic parent that contains the highest H₂O globally (~ 7 wt%), and has evolved by deep crystal fractionation (*Zimmer et al., J.Pet., 2010*), both consistent with a deep magma system (~ 14 km bsl). Do these magmas stall at different depths because of different crustal regimes or because of different parental magmas? Do magmas degas until they physically stall, or do they stall when they start to degas? The answers to these questions bear on how crust is constructed, the volatile budgets at arcs, and the volatile fuel for eruptions.

EarthScope has already invested in several PBO volcano observatories (e.g., Augustine, Akutan, Okmok and Unimak). Future EarthScope and GeoPrisms efforts can target these volcanoes and others to constrain magma movement geophysically and eruptive potential petrologically. Other critical activities include geochronology to constrain the history of volcanism, geochemistry to constrain the origin of the magmas in the subduction zone, geodynamic modeling to constrain modes of magma movement in the crust and eruption dynamics, and seismic experiments to constrain crustal and mantle structure beneath volcanoes.

USArray and EarthScope Science in Alaska Workshop White Paper: An Aleutian Seismological Observatory

S. Prejean¹, J. Power¹, G. Beroza², J. Brown², K. Creager³, A. Ghosh³, J. Gomberg⁴,
C. Thurber⁵, E. Syracuse⁵

1. USGS Volcano Science Center, Alaska Volcano Observatory, Anchorage AK

2. Stanford University, Dept. of Geophysics, Stanford CA

3. University of Washington, Dept. of Earth and Space Sciences, Seattle WA

4. USGS Earthquake Science Center, Seattle WA

5. University of Wisconsin, Dept. of Geoscience, Madison, WI

The Aleutian Islands are an attractive target for dense small-aperture USArray Flexible Array deployments, as volcanic and subduction zone seismicity rates are high but island geography severely limits sub-aerial geophysical data coverage. Akutan and Unalaska Islands are ideal sites for USArray to reach into the Aleutians for six principal reasons: 1. The area has a rich variety of seismic sources at a variety of depths with both tectonic and volcanic origins, 2. The islands are located at the transition between subduction of continental and oceanic lithosphere, near the eastern edge of 1957 M8.6 megathrust rupture zone, 3. Dense array studies would compliment ongoing USGS, AEIC, and PBO monitoring efforts in the region and could potentially dovetail with other multidisciplinary GeoPRISMS and EarthScope projects, 4. Akutan and Makushin are among the most frequently active volcanoes in the United States and are defined as ‘very high threat’ volcanoes by Ewert et al. (2005), 5. Unalaska is the most populated Aleutian Island, and current development of a new airport and geothermal power plant in the region promises continuing growth of critical north Pacific infrastructure here, 6. Unlike some islands in the Aleutians, the field logistics here are tenable, and land use permitting is relatively straight forward as these islands are not classified as wilderness areas.

Dense small-aperture seismic arrays installed on Akutan and Unalaska Islands could potentially have multiple targets. The subduction zone beneath Akutan and Unalaska Islands has been the most prolific producer of detectable deep non-volcanic tremor (NVT) in the Aleutian arc in the past decade (Brown et al., 2011., Peterson et al., 2005). NVT generally locates at the down-dip edge of the 1957 rupture zone (Figure 1). A spectacular case of triggered tremor occurred in this region during the surface wave arrivals of the M 9.0 Tohoku-Oki earthquake (Rubenstein et al., 2011). Despite recent progress in our understanding of NVT in this region, its temporal and spatial extent and relationship to earthquakes and slow slip is not well resolved. Attractive volcanic targets exist in this area as well, which offer excellent opportunities to partner with GeoPRISMS to study the interplay between the subduction zone and volcanic processes in the crust and upper mantle. For example data from dense arrays could be used to refine the velocity tomography of Syracuse et al. (2010). Akutan volcano had the largest seismic response to magmatic intrusion of any Alaskan volcano in the history of local monitoring, when more than 200 earthquakes \leq M 3.5 (M_{\max} 5.1) occurred during a shallow magmatic intrusion in

1996 (Lu et al., 2005). Akutan and Makushin volcanoes are a persistent source of deep (10-45 km) volcanic long-period (LPs) earthquakes as well (Power et al., 2004). The source process and locations of deep LPs are difficult to constrain with data from current seismic networks, yet these events are thought to be related to magma transport. Further study of deep LPs with dense seismic arrays, particularly if tied to geochemical studies, would further our understanding of magma generation and ascent in a volume of crust where these processes are poorly resolved. Deep LPs have the potential to be used as intermediate term precursors to volcanic eruptions.

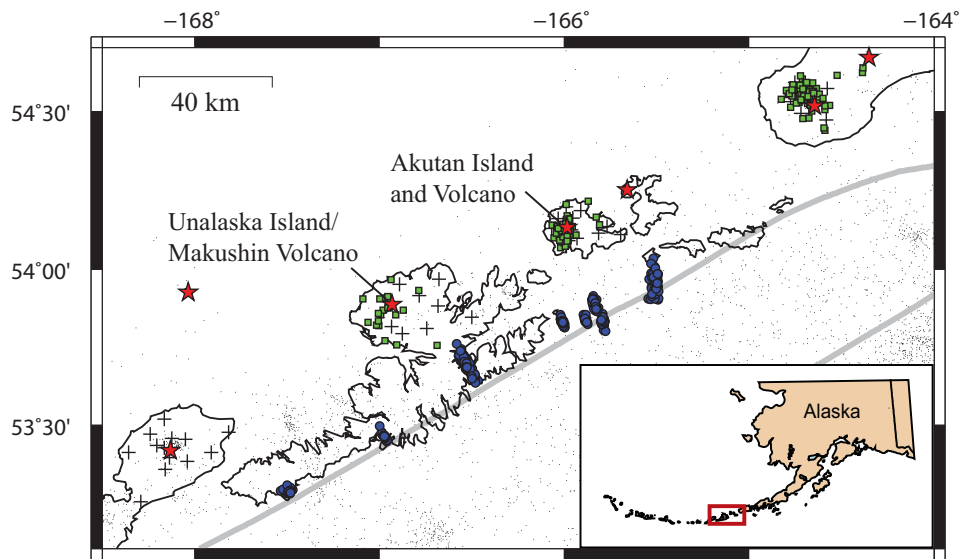


Figure 1 – Target events for small-aperture arrays. Blue circles are locations of low-frequency events within NVT (Brown et al., 2010). Green squares are deep (10-45 km) long period earthquakes. Crosses are existing seismic stations. Red stars are volcano summits. Gray line shows M8.6 1957 rupture zone. Dots show ANSS catalog M2+ earthquake locations 2002-2010. Red box in inset map shows location in Alaska.

Given this suite of seismic targets and following Ghosh et al. (2009, 2011), data from several dense seismic arrays on Akutan and Makushin Islands could potentially refine our understanding of the spatial and temporal characteristics of NVT near the end of a rupture zone, illuminate volcanic system structure and earthquake sources at Akutan and Makushin volcanoes, and constrain the relationship between earthquakes, subducted slab composition and structure, and magma genesis and transport. One advantage of the multi-beam back projection method is that it can track the migrating source, volcanic or non-volcanic, in high resolution over different time scales. We suggest that a suitable Flexible Array deployment in this region could consist of four or more 10-15 sensor arrays located above known NVT and deep LP sources.

- Brown, J.R., S.G. Prejean, G.C. Beroza, J.S. Gombert, and P.J. Haeussler (2010) Evidence for deep tectonic tremor in the Alaska-Aleutian subduction zone, EOS 91, 2010 AGU Fall Meeting.
- Ewert, J.W., M. Guffanti, and T. L. Murray (2005), An Assessment of volcanic threat and monitoring capabilities in the United States: Framework for a National Volcano Early Warning System: USGS Open-File Rep., 2005-1164.
- Ghosh, A., J. E. Vidale, and K. C. Creager (2011) Tremor depth using Array of Arrays in Cascadia, 2011 SSA Annual Meeting.
- Ghosh, A., J. E. Vidale, J. R. Sweet, K. C. Creager, and A. G. Wech (2009), Tremor patches in Cascadia revealed by seismic array analysis, *Geophys. Res. Lett.*, 36, L17316, doi: 10.1029/2009GL039080.
- Lu, Z., C. Wicks, O. Kwoun, J.A. Power, D. Dzurisin (2005), Surface Deformation associated with the March 1996 earthquake swarm at Akutan Island, Alaska, revealed by C-band ERS and L-band JERS radar interferometry, *Can. J. Remote Sensing*, 31, p 7-20.
- Peterson, C., D. H. Christensen, and S. McNutt (2005), Episodic tremor in the Alaska/Aleutian subduction zone, EOS 86, 2005 AGU Fall Meeting.
- Power, J.A., Stihler, S.D., White, R.A., Moran, S.C. (2004), Observations of deep long-period (DLP) seismic events beneath Aleutian arc volcanoes; 1989-2002, *J. Volcanol. and Geotherm. Res.*, 138, p. 243-266.
- Syracuse, E.M., C.H. Thurber, J.A. Power, and S.G. Prejean (2010) Three-dimensional velocity structure and high-precision earthquake relocations at Augustine, Akutan, and Makushin Volcanoes, Alaska, EOS 91, 2010 AGU Fall Meeting.
- Rubenstein et al., (2011) Widespread triggering of earthquakes and tremor by the 2011 M9.0 off-Tohoku earthquake, 2011 SSA Annual Meeting.

What are the relative roles of crustal strength versus plate driving forces in Alaska tectonics?

Roeske, Sarah Geology Dept. University of California, Davis
smroeske@ucdavis.edu

Saltus, Richard U.S. Geological Survey, Denver saltus@usgs.gov

Our understanding of plate driving forces continues to be challenged by data from wide zones of continental deformation at convergent margins. The northern Cordillera, in particular the western Yukon, across Alaska and into Siberia, can broadly be considered a plate boundary zone and active tectonics impact the region as far as 1200 km in from the trench. This region is a textbook place to study the wide range of variables that control continental deformation, in particular the role of plate boundary interactions, mantle flow, and crustal rheology.

The coupling of the subducting Pacific plate and Yakutat block with the overriding plate clearly plays a major role, because the subducting slab is very low angle and buoyant mafic crust of the Yakutat block is involved, but this does not explain deformation in the northern and western half of the state. Mantle flow on the base of the lithosphere also clearly plays a role, but this too would appear to affect primarily the southern part of the state, in particular the eastern edge of the slab. Deformation beyond the edge of the subducting slab, which is approximately everything north of the Denali fault, must be occurring due to some combination of mantle drag and plate boundary coupling. How those forces are transferred to distant corners of the state remains a major question.

The diverse nature of the Alaskan crust, both in composition and thickness, and the presence of long-lived rheologic boundaries expressed as large-scale strike-slip faults, locally has a profound influence on the focusing of crustal strain. Strands of Mesozoic–early Cenozoic dextral faults in northern and central Alaska, including the Kobuk, Kaltag, Tintina, and Hines Creek and McKinley strands of the Denali fault, show Quaternary activity. In other regions, such as the northeast corner of the state near the margin with the Canada basin, it is less obvious what is causing the localized strain. The Arctic Alaska subplate seems to represent a thick, cold block, but it is not clear how that connects to the Siberian and North American craton. Blocks of mafic (on the surface) crust south of the Arctic Alaska subplate include the Yukon-Koyukuk basin and Yukon flats; potential field indicates they are not normal ocean crust, but they play the role of relatively rigid bodies regionally. They would appear to play a role in transferring stress from the diffusively deforming central interior, between the Denali and Tintina faults, to the North Slope.

Our current knowledge of the crustal character of Alaska is based on a blend of potential field and regional mapping (scales of 1:250,000 and smaller). Large swaths of interior and western Alaska are heavily vegetated, so the sparse geophysical transects (TACT and BEAAR) have been key in helping us interpret the potential field results. Earthscope's potential to resolve the thickness of the lithosphere and crust and help constrain its velocity will answer first-order tectonic questions that are relevant to Alaska, and because of the diverse nature of the tectonics the results will elucidate other studies of diffuse continental deformation.

Local stress field changes accompanying episodes of volcano-seismic unrest in the eastern Aleutians: An overview of results and unresolved questions

D.C. Roman^{1,2}, J. O'Brien¹, M. Gardine^{1,2}, W.W. Kilgore¹

1. Department of Geology, University of South Florida

2. Department of Terrestrial Magnetism, Carnegie Institution of Washington

The eastern Aleutians have proven to be an excellent natural laboratory for understanding seismological signatures of volcanic unrest. First, there have been numerous seismic swarms at Cook Inlet volcanoes in the past 20 years, some of which have preceded eruptions, and some of which did culminate in eruption (and possibly represented shallow crustal intrusions). One particularly enigmatic swarm occurred in the Denali Volcanic Gap, and was not associated with an existing volcanic vent. Second the volcanoes of the Cook Inlet are relatively well-instrumented, with permanent networks of 6-12 short-period seismometers operated by the Alaska Volcano Observatory.

Detailed analyses of double-couple fault-plane solutions (FPS) from several major earthquake swarms have been used to investigate processes of near-surface magma intrusion and migration. In several cases, $\sim 90^\circ$ horizontal rotations of maximum compressive stress were found to precede eruptions and accompany non-eruptive seismic swarms. These include the nine-month-long swarm leading up to the 1992 eruptions of Crater Peak, a non-eruptive swarm at Crater Peak in Nov 1992, a short precursory swarm preceding the 2009 Redoubt eruption, and a short non-eruptive swarm at Mt. Martin in the Katmai Volcanic Cluster in 2006. In contrast, there was no evidence for local stress field rotation during a strong non-eruptive swarm at Iliamna Volcano in 1996 that was accompanied by significantly elevated SO_2 and CO_2 emissions. Finally, it could not be determined whether a local stress field reorientation occurred during a strong swarm that occurred near Strandline Lake, ~ 30 km northeast of Mt. Spurr in the Denali Volcanic gap, in 1996, because the orientation of the background stress field in this region is poorly characterized.

Based on the results of the studies described above, fault-plane solution analysis appears to be a promising method of eruption forecasting in the Cook Inlet regions and possibly elsewhere in the Aleutians. This approach has the potential to provide early confirmation of conduit pressurization during the initial stages of volcano-seismic unrest, and can be adapted for near-real-time analysis in an observatory environment. However, two $\sim 90^\circ$ stress field rotations associated with non-eruptive unrest (at Crater Peak in November 1992 and Mt. Martin in 2006) indicate the potential for false positives based on FPS analysis. Furthermore, knowledge of the local background stress field appears to be critical for interpreting swarm FPS: At Mt. Martin in 2006, a near-isotropic background stress field may have resulted in a detectable stress field rotation due to a small-volume intrusion of magma. Conversely, at Iliamna 1996, a strongly deviatoric background stress field may have prevented the occurrence of a local stress field rotation due to a small volume intrusion. Finally, at Strandline Lake in 1996, it unclear whether there was a rotation or not because the orientation of the background (non-rotated) stress field is unknown.

Denser seismic instrumentation throughout the Cook Inlet region will allow for more in-depth swarm FPS analysis, including analysis of FPS for lower magnitude and/or deeper earthquakes that may help to address the issue of 'false positive' local stress field reorientations. In addition, a dense network of seismic instruments in this region of Alaska would allow for better characterization of local background stress field orientations through analysis of shear-wave splitting in lower crustal earthquakes and calculation of well-constrained FPS for local background earthquakes.

Crustal Seismicity in the Aleutian Arc and Implications for Arc Deformation

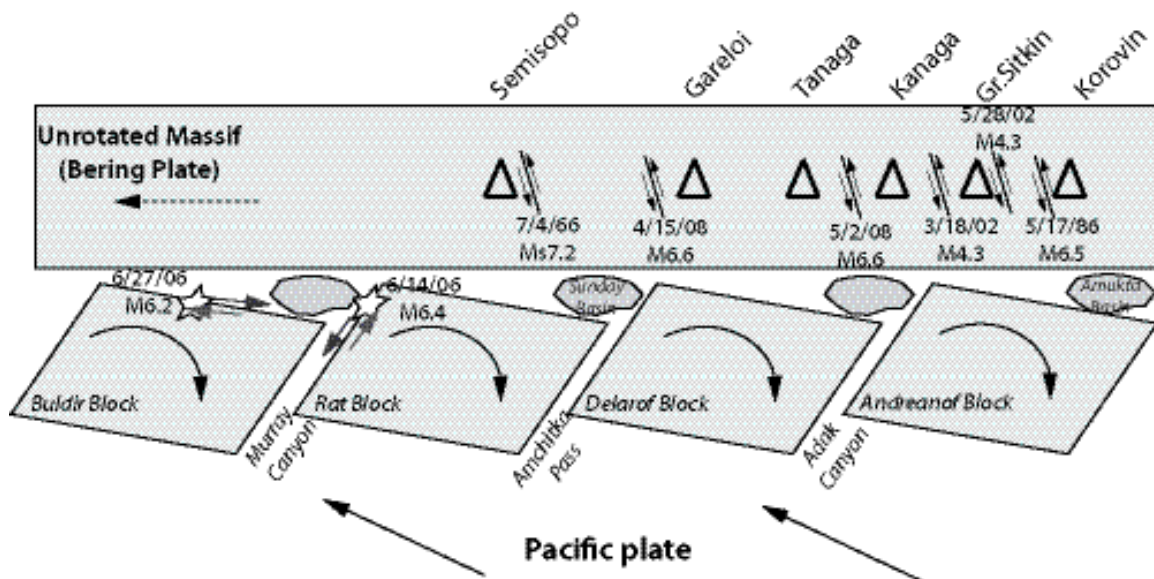
Natalia A. Ruppert

Geophysical Institute, University of Alaska Fairbanks

Central and Eastern Aleutian Arc is characterized by oblique convergence between the subducting Pacific and overriding Bering Plates. This results in westward translation of the arc and formation of rotating crustal blocks in the forearc. In 2006-2010 several moderate shallow crustal earthquakes (up to magnitude 6.7) occurred in the region. These events were located about 150 km away from the trench, on the volcanic axis, and had either strike-slip (west of 174°W) or normal (east of 174°W) faulting mechanisms. Prior to 2006, several similar events can be found in the literature and earthquake catalogs.

Two of the recent earthquakes are associated with faulting along the boundaries of rotating crustal blocks. The 27 June 2006 magnitude 6.2 earthquake occurred along the northern boundary of the Buldir block and the 14 June 2006 magnitude 6.4 earthquake occurred along the boundary between the Buldir and Rat blocks. Majority of the other strike-slip crustal earthquakes (e.g., 1966, 1986, 2008) occurred on NNW-striking faults in the unrotated part of the Bering massif. They may be manifestation of Riedel shearing in the region north of the blocks. Such shears are usually arranged en echelon, at inclinations between 10 and 30 degrees to the direction of relative plate motion. Normal faulting crustal earthquakes east of 174°W manifest extension of the arc in response to the arc curvature and obliquity of convergence.

This type of faulting is not unique to the Aleutian Arc. Similar events were reported in the Banda Arc, Nicaragua and Kurile Arc. Thus, additional investigations of crustal earthquakes in the Aleutians may shed more light onto arc deformation that may be applicable to other regions around the globe.



Crustal Seismicity in the Mainland Alaska and Its Relation to Active Faults and Crustal Blocks

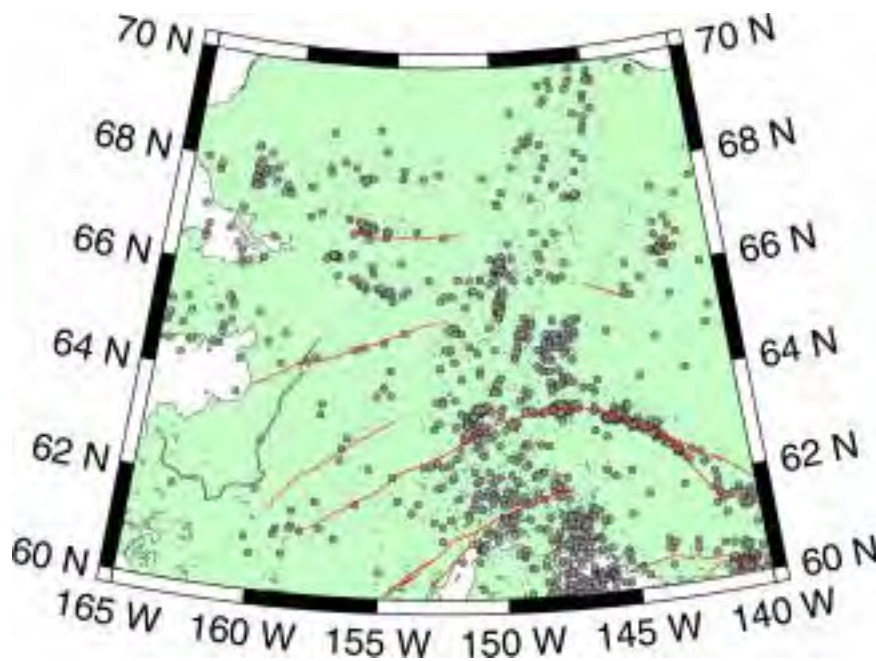
Natalia A. Ruppert

Geophysical Institute, University of Alaska Fairbanks

The interaction of the Pacific and North American plates along the Alaskan southern margin and the Aleutian arc is the first order, driving force for Alaskan tectonics. A transform boundary between the plates in southeastern Alaska lies long the Queen Charlotte-Fairweather fault system. Additional complications are imposed by the ongoing collision of the Yakutat block in the transition zone between the convergent and transform plate boundaries. While about 99% of the historic seismic moment release in Alaska occurred along the major plate interface, active crustal seismicity belts and active surface structures extend far into the continental part of Alaska, as far north and west as the Beaufort and Bering sea. There were about 40 crustal events in the past 100 years in the mainland Alaska with magnitudes between 6 and 8. Seven of these had magnitudes of 7 or greater. I.e., the rate of occurrence is one M6+ crustal earthquake every 2-3 years.

GPS velocities of the sites in interior Alaska move somewhat differently than would be expected for a "stable plate" interior, indicating that the Alaskan part of the North American plate is internally deforming. A number of crustal blocks (or microplates) of various extent have been suggested to explain crustal motions, seismicity distribution and the resulting deformation in Alaska beyond the immediate vicinity of the major plate boundary. The best documented examples include the Bering and the Wrangell blocks. An unresolved problem is to identify the boundaries and relative motions of these blocks. The boundaries of these crustal blocks apparently are not simple linear structures but rather broad zones of distributed deformation.

The seismicity and deformation across this broad region, and the forces that drive them, are not well understood. Additional investigations into crustal deformation and seismicity would greatly improve understanding of active tectonics in Alaska.



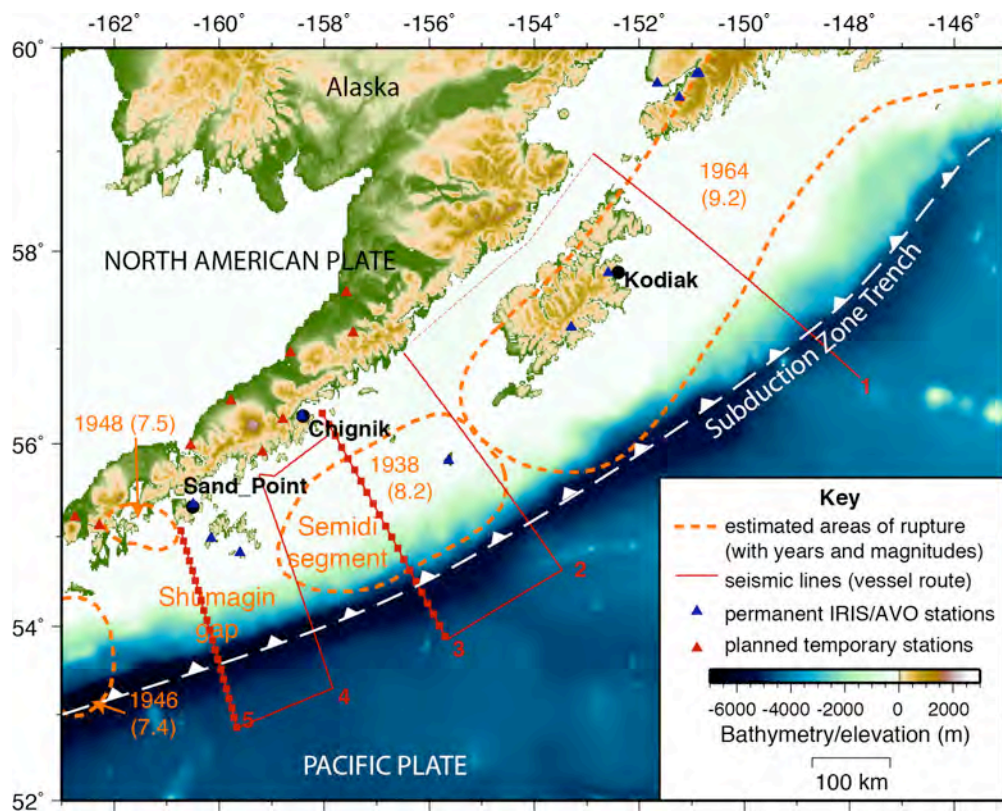
Crustal seismicity in Alaska from AEIC Earthquake Catalog 1898-present (points - magnitude 3 and greater, circles - magnitude 4.0 and greater). Red lines are major active faults.

Upcoming active-source seismic study of the Alaska megathrust

Donna J. Shillington¹, Mladen Nedimović^{1,2}, Spahr Webb¹, Katie Keranen³

¹Lamont-Doherty Earth Observatory of Columbia University, Palisades, NY, ²Dalhousie University, Halifax, Nova Scotia, ³University of Oklahoma, Norman, OK

In July-August 2011, we plan to acquire a large onshore-offshore active-source dataset focused on the Semidi segment of the Alaska/Aleutian subduction zone, which last ruptured in 1938 in a M8.2 event. The primary goal of this project is to use seismic reflection and refraction data to constrain properties at the megathrust, in particular the downdip limit of the seismogenic zone, using deep-penetration seismic reflection data. The nearer the landward end of the seismogenic zone lies to the coast, the larger and longer the onshore strong ground motions will be (Peterson et al., 2002). Previous work on the Cascadia margin suggests that changes in seismic reflection properties can be used to differentiate between locked and sliding parts of the plate boundary (Nedimović et al., 2003), and studies of other subduction zones hint at similar relationships (Kodaira et al., 2005; Groß et al., 2008; Bell et al., 2010). However, many of these investigations have been done in areas with poorly known rupture histories and/or require the knitting together of onshore and offshore seismic datasets to examine the downdip extent of the seismogenic zone. Alaska is an excellent target for this program because virtually the entire Alaska-Aleutian megathrust has ruptured in large to great earthquakes in the last century (Davies et al., 1981) and the entire locked zone appears to lie offshore, allowing continuous marine profiling of its full extent.



Map of planned experiment. Red lines and squares indicate planned MCS lines and OBS locations, respectively, and red triangles indicate planned location of temporary onshore stations. Estimated rupture areas from Davies et al., 1981.

The megathrust also appears to exhibit significant along-strike variations in current coupling in our study region, from freely slipping in Shumagin Gap to fully locked in the Semidi segment (e.g., Freymueller and Beavan, 1999; Fournier and Freymueller, 2007). Another goal of our program is to examine changes in subduction parameters and fault properties associated with these along-strike changes in fault behavior.

Our experiment will involve the acquisition of deep-penetration seismic reflection data along a series of dip profiles using two 8-km (640-channel) streamers and the full 6600 cu in. air gun array of the R/V *Marcus Langseth*. Our profiles will survey the center and edges of the Semidi segment, the Shumagin Gap and a region that ruptured in the 1964 M9.2 Good Friday event. Wide-angle seismic reflection/refraction data will be acquired with closely spaced short-period OBS deployed on two of the profiles. Nine broadband instruments will also be deployed onshore for two months this summer and will record the entire active-source experiment, thereby extending ray coverage to deeper levels of the subduction zone, as well as local and teleseismic earthquakes.

- Bell, R., R. Sutherland, D. H. N. Barker, S. Henrys, S. Bannister, L. Wallace, and J. Beavan, Seismic reflection character of Hikurangi subduction interface, New Zealand, in the region of repeated Gisborne slow slip events, *Geophys. J. Intl.*, **180**, 34-48, 2010.
- Davies, J. N., Sykes, L. R., House, L. and Jacob, K., Shumagin seismic gap, Alaska peninsula: History of great earthquakes, tectonic setting, and evidence for high seismic potential, *J. Geophys. Res.* **86**, 3821-3855, 1981.
- Fournier, T.J., and Freymueller, J.T., Transition from locked to creeping subduction in the Shumagin region, Alaska: *Geophys. Res. Lett.*, **34**, L06303, doi: 10.1029/2006GL029073, 2007.
- Freymueller, J. T. and Beavan, J., Absence of strain accumulation in the western Shumagin segment of the Alaska subduction zone, *Geophys. Res. Lett.* **21**, 3233-3236, 1999.
- Groß, K., Micksch, U., and TIPTEQ Research Group, Seismics Team, The reflection seismic survey of project TIPTEQ - the inventory of the Chilean subduction zone at 38.2°S: *Geophys. J. Intl.*, **172**, p. 565-571, 2008.
- Kodaira, S., Iidaka, T., Nakanishi, Park, J-O., Iwasaki, T. and Kaneda, Y., Onshore-offshore seismic transect from the eastern Nankai Trough to central Japan crossing a zone of the Tokai slow slip event, *Earth Planets Space* **57**, 943-959, 2005
- Nedimović, M. R., Hyndman, R. D., Ramachandran, K. and Spence, G. D., Reflection signature of seismic and aseismic slip on the northern Cascadia subduction interface, *Nature* **424**, 416-420, 2003.
- Peterson, M.D., Cramer, C.H. and Frankel, A.D., Simulations of seismic hazard for the Pacific Northwest of the United States from earthquakes associated with the Cascadia subduction zone, *Pure and Applied Geophysics*, **159**, 2147-2168, 2002.

FlexArray Alaska: Seismic imaging of major sedimentary basins overlying the subducting Pacific–Yakutat slab

Carl Tape¹, Stéphane Rondenay², Doug Christensen¹

¹ Geophysical Institute, University of Alaska Fairbanks, Fairbanks, Alaska, USA

² Massachusetts Institute of Technology, Cambridge, Massachusetts, USA

May 6, 2011

Abstract

Sedimentary basins represent some of the strongest heterogeneity on Earth. For example, wave speed differences from unconsolidated sediments in the basins ($V_S \approx 200$ m/s) to an adjacent exhumed batholith ($V_S \approx 2000$ m/s) may vary by as much as an order of magnitude. Just as the heterogeneity in the crust creates complications for global seismic studies, the heterogeneity of sedimentary basins creates complications for crustal and upper mantle seismic studies. These sedimentary basins trap seismic energy, thereby obscuring subtle signals that originate from target structures below (e.g., core-mantle boundary, upper mantle discontinuity, Moho). Basins in the vicinity of population centers elevate the seismic hazard by their amplification and prolongation of seismic shaking.

Our proposal is aimed at “top-down” imaging of two regions of the Alaska subduction zone, with the simple reasoning that by first isolating the strongest heterogeneity of the basins, we can better image the lower crust and upper mantle heterogeneity associated with subduction. A FlexArray deployment covering two distinct portions of the Alaska subduction zone would play a critical role in understanding the relationships among subducting slabs, upper mantle flow, and active sedimentary basins.

Fundamental objectives

1. What is the 3D structure and broadband seismic response of the Cook Inlet and Nenana basins (Figures 1–3)?
2. What is the 3D structure of the subducting Pacific–Yakutat slab in the vicinity of each basin?
3. How is the formation of the sedimentary basins related to the dynamics of the subduction zone?
4. What is the anisotropic structure: (1) below the slab, (2) within the slab, and (3) above the slab?
5. How can we improve seismic imaging techniques in the presence of major sedimentary basins?
6. What are the modes of deformation inferred from source mechanisms of local intraslab and crustal earthquakes?

Scientific tasks

1. Build an initial 3D upper mantle and crustal model of the subduction zone in Alaska.
2. Build an initial high-resolution 3D model of the crust and upper mantle in the vicinity of the Cook Inlet basin.
3. Build an initial high-resolution 3D model of the crust and upper mantle in the vicinity of the Nenana basin.

4. Collect 2–3 years of waveform data. Motivated by reducing costs and utilizing natural pathways, we have proposed a multi-transport deployment of 38 stations (22 Cook Inlet, 16 Nenana). 27 of the stations have no road access and would be approached with by boat (ocean, lake, or river), fixed-wing (Interior lakes), or helicopter (subduction profile).
5. Use spectral-element and adjoint methods within a tomographic inversion to iteratively improve the high-resolution 3D models (*Tape et al.*, 2009).
6. Use local shear-wave splitting to determine anisotropic structure in the mantle wedge or crust. Compare with previous SKS splitting results (*Christensen and Abers*, 2010).
7. Use generalized radon transform or receiver function analysis to identify primary interfaces (Moho, slab), in addition to those within the upper mantle and crust. Such techniques have proven successful on Alaska data sets (*Ferris et al.*, 2003).
8. Investigate the relationships among slab seismicity, crustal seismicity, gravity anomalies, and the formation of the basins (e.g., *Wells et al.*, 2003; *Haeussler and Saltus*, 2011).
9. Investigate the effects of topography on seismic waves. The Cook Inlet subduction profile contains the Harding Ice Field, as well as Mt. Redoubt (active volcano) and other mountains. We expect the topography to influence the wavefield, at least at shorter periods.
10. Perform targeted 2D and 3D imaging of the Cook Inlet subducting slab (e.g., *Rondenay et al.*, 2008). What can the images (in combination with seismicity) tell us about the compositional and thermal structure of the slab?

References

- Christensen, D., G. Abers, and J. Freymueller (2008), Multidisciplinary observations of subduction (MOOS) experiment in south-central Alaska, in *EOS Trans. Am. Geophys. Un.*, vol. 89(53), Abstract U51B-0041.
- Christensen, D. H., and G. A. Abers (2010), Seismic anisotropy under central Alaska from SKS splitting observations, *J. Geophys. Res.*, 115, B04315, doi:10.1029/2009JB006712.
- Ferris, A., G. A. Abers, D. H. Christensen, and E. Veenstra (2003), High resolution image of the subducted Pacific (?) plate beneath central Alaska, 50–150 km depth, *Earth Planet. Sci. Lett.*, 214, 575–588.
- Haeussler, P. J., and R. W. Saltus (2011), Location and extent of Tertiary structures in Cook Inlet basin, Alaska, and mantle dynamics that focus deformation and subsidence, in *Studies by the U.S. Geological Survey in Alaska 2008–2009*, edited by J. A. Dumoulin and J. P. Galloway, p. 26, U.S. Geol. Survey, Washington, D.C., Professional Paper 1776-D.
- Rondenay, S., G. A. Abers, and P. E. van Keken (2008), Seismic imaging of subduction zone metamorphism, *Geology*, 36(4), 275–278.
- Saltus, R. W., P. J. Brown II, R. L. Morin, and P. L. Hill (2008), 2006 Compilation of Alaska Gravity Data and Historical Reports, U.S. Geol. Survey Digital Series 264, CD-ROM.
- Shellenbaum, D. P., L. S. Gregersen, and P. R. Delaney (2010), Top Mesozoic unconformity depth map of the Cook Inlet Basin, Alaska, Alaska Division of Geological & Geophysical Surveys Report of Investigation 2010-2, 1 sheet, scale 1:500,000.
- Tape, C., Q. Liu, A. Maggi, and J. Tromp (2009), Adjoint tomography of the southern California crust, *Science*, 325, 988–992.
- Wells, R. E., R. J. Blakely, Y. Sugiyama, D. W. Scholl, and P. A. Dinterman (2003), Basin-centered asperities in great subduction zone earthquakes: A link between slip, subsidence, and subduction erosion?, *J. Geophys. Res.*, 108(B10), 2507, doi:10.1029/2002JB002072.

Slab seismicity (depth > 40 km), 1990 to 2010, $M \geq 3.0$

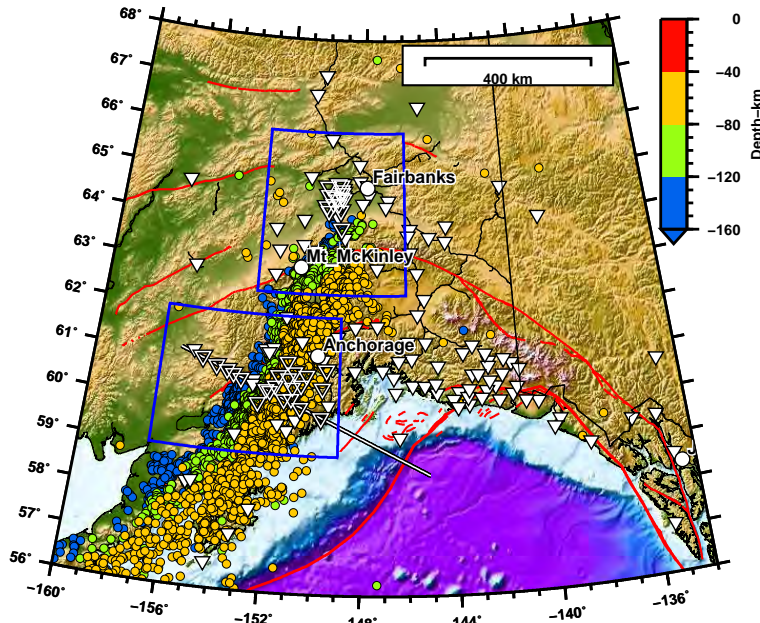


Figure 1: Slab seismicity of Alaska, indicated by earthquake depths greater than 40 km. Inset boxes are shown in Figures 2 and 3. Filled white triangles denote broadband stations in Alaska; open white triangles denote proposed FA stations.

Southern Alaska and Cook Inlet Basin

Slab seismicity (depth > 40 km), 1990 to 2010, $M \geq 3.0$

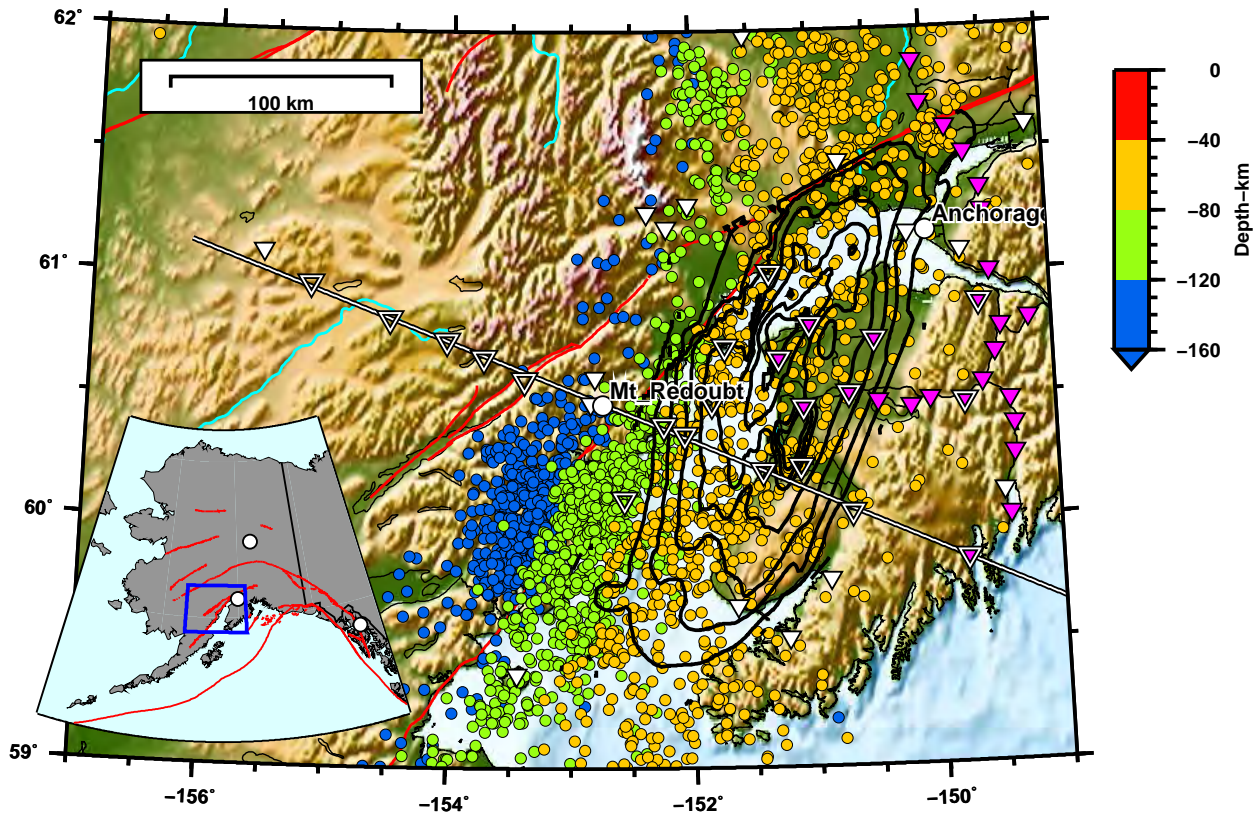


Figure 2: Slab seismicity and station coverage in the Cook Inlet region. Contours mark the Tertiary basement of the Cook Inlet basin (*Shellenbaum et al., 2010*). Open triangles denote proposed FA stations; some of these reoccupy previous MOOS station sites (magenta) (*Christensen et al., 2008*). The white line, passing through Redoubt volcano, denotes a 2D profile for target studies of the slab.

Interior Alaska and Nenana Basin

Crustal and slab seismicity, 1990 to 2010, $M \geq 3.0$

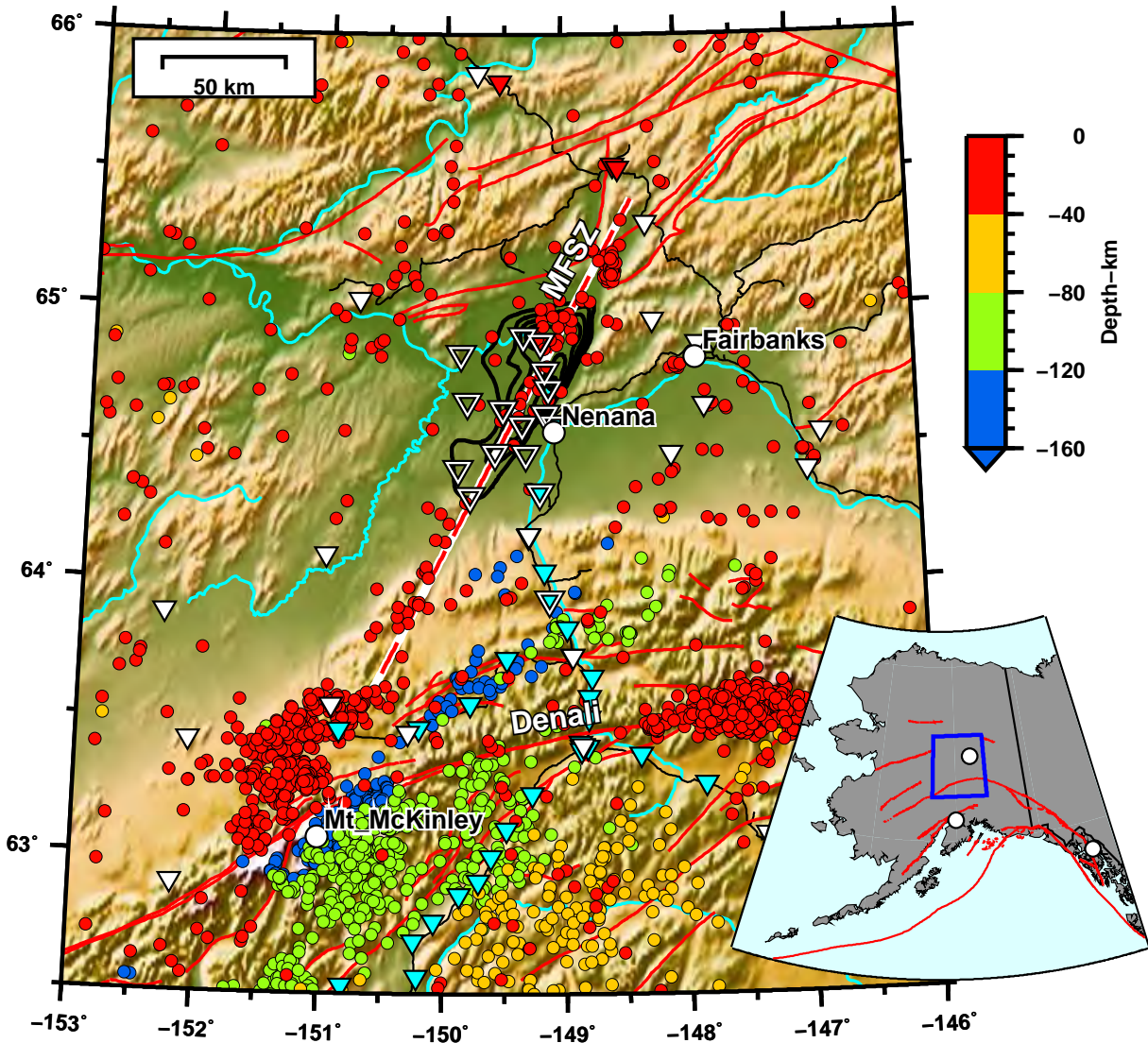


Figure 3: Slab and crustal seismicity and station coverage in central Alaska. Note that the slab seismicity ends at the latitude of the southern extent of the Nenana basin, which is marked by free-air gravity low contours (*Saltus et al.*, 2008). The red dotted line denotes the Minto Flats Seismic Zone, which parallels the strike of the Nenana basin and extends toward Mt. McKinley. Open triangles denote proposed FA stations; some of these reoccupy previous BEAAR station sites (cyan) (*Ferris et al.*, 2003).

Toward a multiscale seismic velocity model for Alaska

Carl Tape

Geophysical Institute, University of Alaska Fairbanks, Fairbanks, Alaska, USA

May 6, 2011

Overview

Seismic velocity structure is a fundamental characteristic of any given region. Seismic velocity models provide a starting point for iterative seismic tomographic inversions, whereby the velocity models are improved while minimizing differences between observed and synthetic seismograms. The success of the tomographic inversion is driven by three features: (1) the availability and quality of observed data; (2) the accuracy of the forward model to compute synthetic seismograms; (3) the accuracy of the inverse model.

The availability of data in Alaska motivates the underlying multiscale nature of the seismic velocity model. For example, we might classify target structures into five scales:

1. Scale of 3000 km: global (core + mantle).
2. Scale of 300 km: the subduction system (upper mantle, subducting slabs).
3. Scale of 30 km: crust.
4. Scale of 3 km: sedimentary basins and volcanoes.
5. Scale of 300 m: glaciers, fault zones, and sub-horizontal layers (e.g., active source surveys).

Our objective is to interrogate and improve seismic velocity models using 2D and 3D wavefield simulations. The *computational scale* for each target structure is approximately the same. For example, the computational cost to simulate a 10 Hz wavefield from a marine refraction survey (Figure 3) is comparable to simulating the global wavefield for a M_w 9.2 earthquake (Figure 2). Thus, our model parameterization must reflect our desire for variable resolution.

The wavefield simulations may be used within an adjoint-based inverse problem, as demonstrated extensively for the southern California crust (e.g., *Tape et al.*, 2009). Future efforts in Alaska will involve assembling different structural and seismic data to construct a reference 3D seismic velocity model (e.g., *Eberhart-Phillips et al.*, 2006; *Fuis et al.*, 2008). This approach of constructing, validating, and refining 3D velocity models has been developed by the Southern California Earthquake Center over the past decade (Figure 1).

Fundamental objectives

1. To develop a 3D seismic velocity model for Alaska that agrees with (most) available data sets (seismic and non-seismic) and is adapted to multiple scales.
2. To provide an easy, functioning delivery method for the model for all users.
3. To establish a computational platform for validating and improving the model with direct comparisons between observed and simulated seismograms.

References

- Christeson, G. L., S. P. S. Gulick, H. J. A. van Avendonk, L. L. Worthington, R. S. Reece, and T. L. Pavlis (2010), The Yakutat terrane: Dramatic change in crustal thickness across the Transition fault, Alaska, *Geology*, *38*(10), 895–898.
- Eberhart-Phillips, D., D. H. Christensen, T. M. Brocher, R. Hansen, N. A. Ruppert, P. J. Haeussler, and G. A. Abers (2006), Imaging the transition from Aleutian subduction to Yakutat collision in central Alaska, with local earthquakes and active source data, *J. Geophys. Res.*, *111*, B11303, doi:10.1029/2005JB004240.
- Fuis, G. S., et al. (2008), Trans-Alaska Crustal Transect and continental evolution involving subduction underplating and synchronous foreland thrusting, *Geology*, *36*(3), 267–270.
- Plesch, A., C. Tape, J. H. Shaw, and members of the USR working group (2009), CVM-H 6.0: Inversion integration, the San Joaquin Valley and other advances in the community velocity model, in *2009 Southern California Earthquake Center Annual Meeting, Proceedings and Abstracts*, vol. 19, pp. 260–261.
- Süss, M. P., and J. H. Shaw (2003), P-wave seismic velocity structure derived from sonic logs and industry reflection data in the Los Angeles basin, California, *J. Geophys. Res.*, *108*(B3), 2170, doi: 10.1029/2001JB001628.
- Tape, C., Q. Liu, A. Maggi, and J. Tromp (2009), Adjoint tomography of the southern California crust, *Science*, *325*, 988–992.

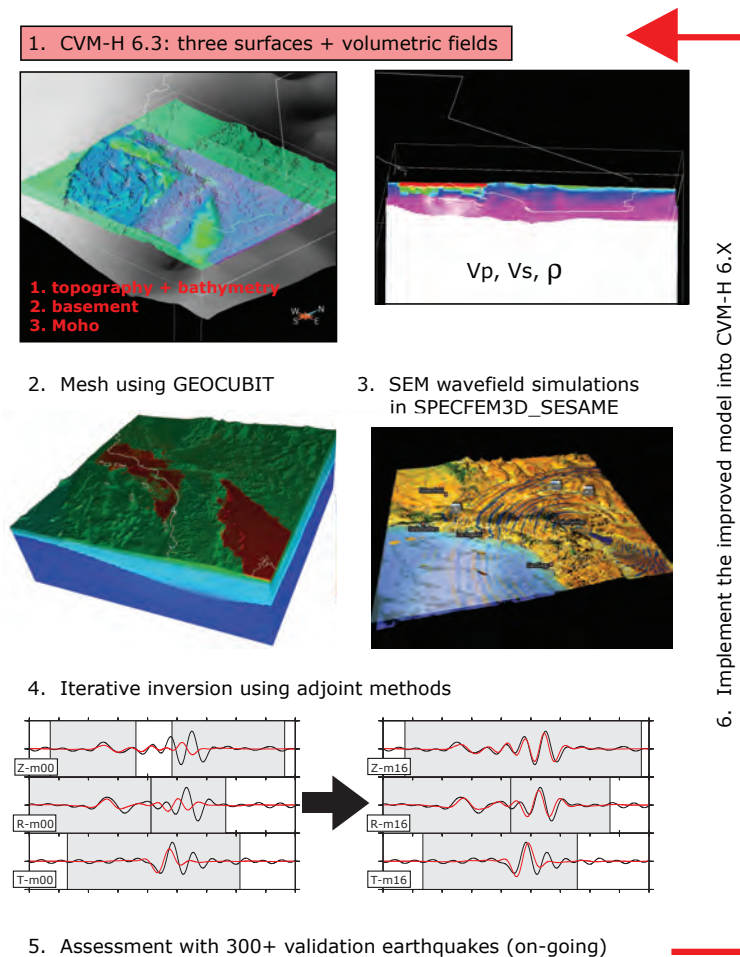


Figure 1: Workflow for construction and improvement of 3D seismic velocity models, with southern California as an example (Süss and Shaw, 2003; Plesch et al., 2009).

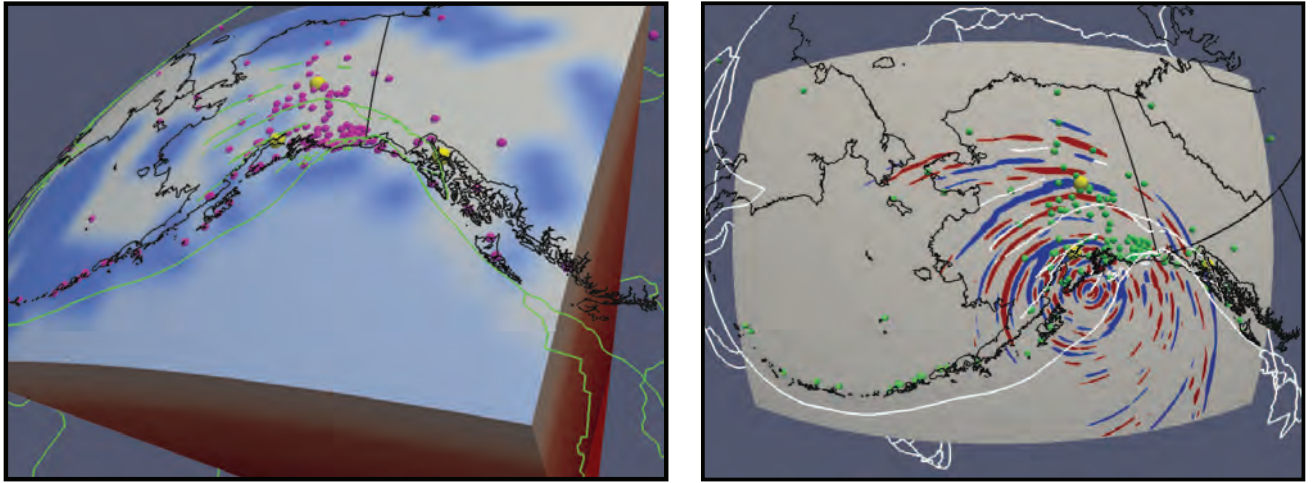


Figure 2: (Left) Global-scale simulations of earthquakes within the 3D tomographic model S40RTS combined with the crustal model Crust2.0. (Right) Snapshot from a wavefield simulation of a M_w 9.2 scenario earthquake on the Aleutian megathrust. Accurate structural models are needed to improve the predicted ground displacements for such earthquakes.

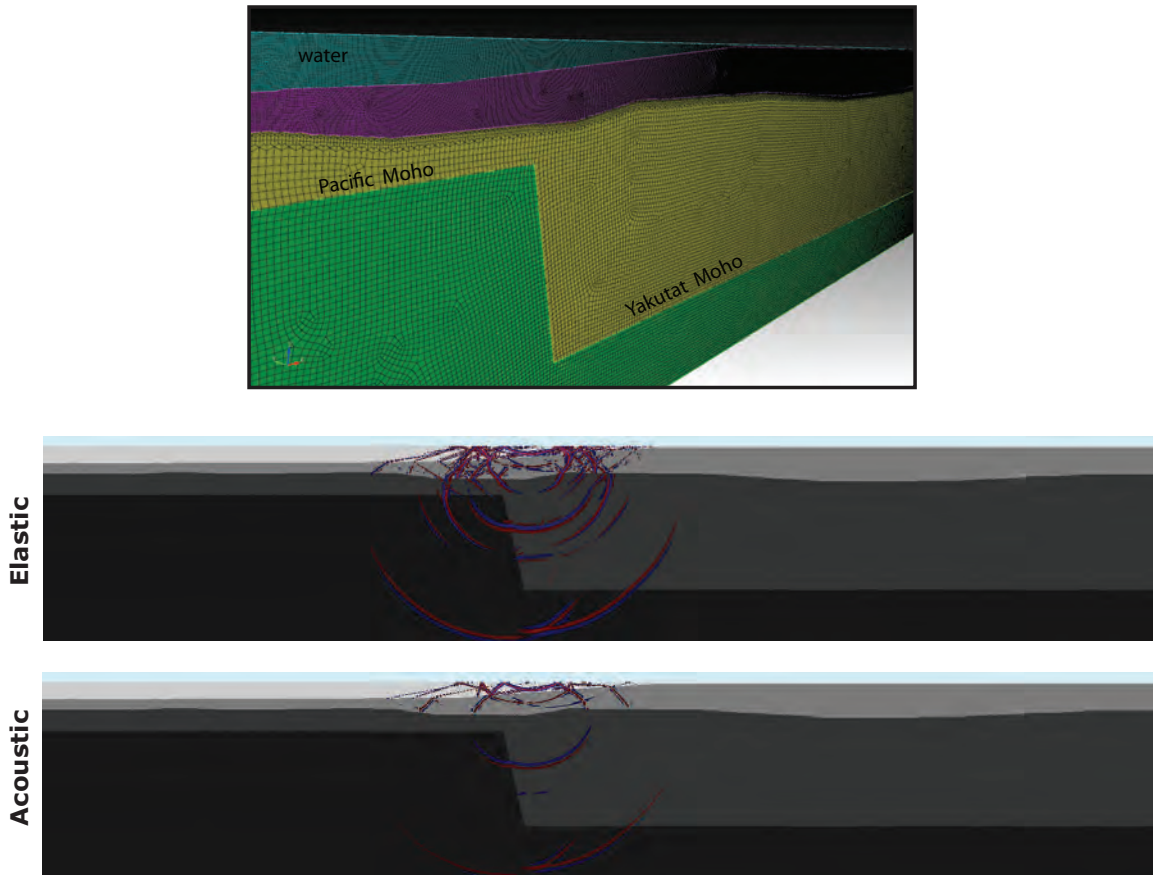


Figure 3: (Top) Oblique view of a 2D mesh for the model of *Christeson et al.* (2010). The element sizes depend on the average V_P and V_S in each of four units: water, sediments + sedimentary rock, rock, and mantle. The Moho step is $\Delta z = 21.8$ km. (Bottom) Elastic and acoustic wavefield snapshots at time $t = 8$ s following an acoustic source near the water surface.

Quantifying the Influence of Sea Ice on Ocean Microseism

Victor C. Tsai and Daniel E. McNamara

Geologic Hazards Science Center, United States Geological Survey

Microseism is potentially affected by all processes that alter ocean wave heights. Because strong sea ice prevents large ocean waves from forming, sea ice can therefore strongly affect microseism amplitudes. This suggests the possibility of monitoring sea ice strength using microseism. Seismic stations in Alaska that surround the Bering Sea (which is seasonally covered by sea ice) are perfectly situated to allow quantification of this link between sea ice and microseism. Preliminary work (Tsai and McNamara, in prep.) shows that there is indeed a large and quantifiable sea ice signal, as shown in the figure below. Station UNV, which is south of the southernmost extent of sea ice, is unaffected by sea ice and the PSD variability is typical of traditional ocean microseism variability. On the other hand, station TNA, located on the Seward Peninsula, is locally surrounded by sea ice between December and May of each year. There is a notable drop in short-period microseism power associated with exactly these times during which sea ice is present locally and dampens the ocean waves responsible for short-period microseism. Unfortunately, one difficulty in quantifying this signal is the lack of high-quality continuous seismic stations surrounding the Bering Sea. In fact, only four stations within the Alaska Regional Seismic Network are well situated, and two of these have many glitches that make it difficult to use. EarthScope presents an unprecedented opportunity to expand progress in this area.

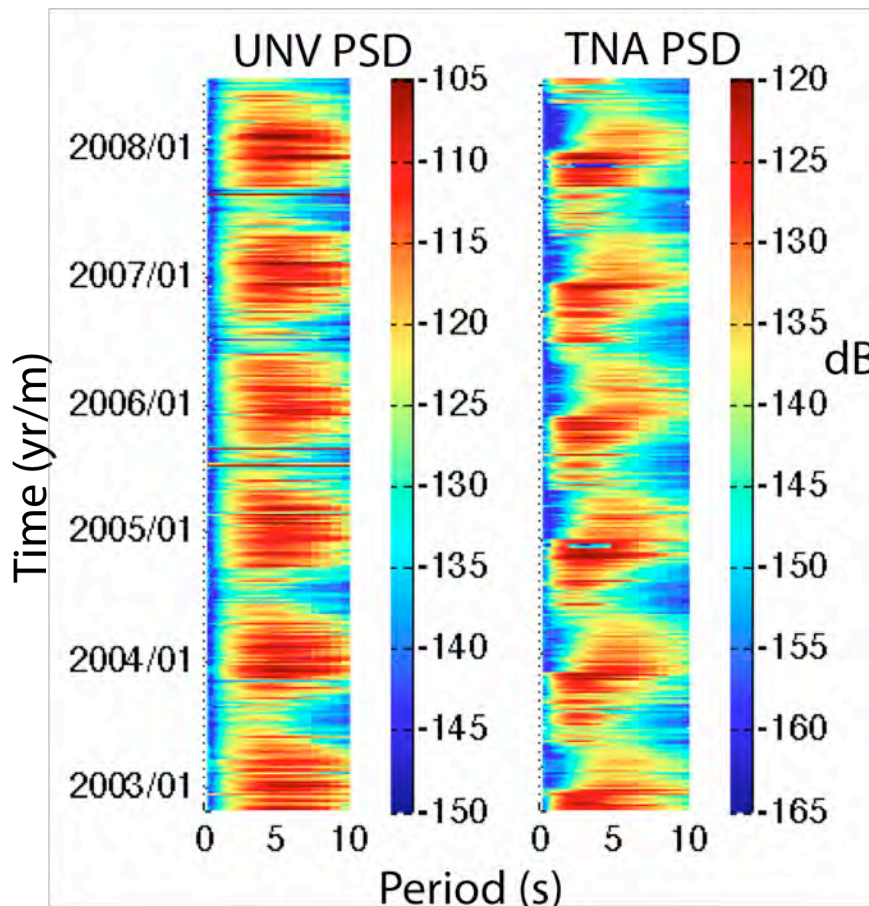


Figure 1: Spectrograms of power spectral density (PSD) (in dB) for two stations in the Bering Sea. UNV (Unalaska Valley) is located in the Aleutian Island chain, and is unaffected by sea ice. TNA (Tin City, Alaska) is located on the Seward Peninsula and is affected by sea ice between December and May of each year.

Earthquake occurrence rate in Alaska 1960-2010

Michael West, mewest@alaska.edu
Geophysical Institute, Univ. Alaska Fairbanks

The Alaska earthquake catalog has improved over the past century reflecting technical advances in instrumentation and data analysis. The 1964 Good Friday earthquake was a turning point. Following the catastrophic magnitude 9.2 event, the catalog is complete down to about magnitude 5, improving to magnitude 3 by the early 1970s. By this time, Mb and Ms were supplementing local magnitudes for most events above magnitude 4.

Beginning in 1976 the global CMT project began contributing Mw magnitudes for events 5 and greater. Moment magnitudes generated by the Alaska Earthquake Information Center, beginning in 2002, brought the Mw threshold closer to 4.

Over the past 50 years, the Alaska region has generated an average of 150 earthquakes per year of magnitude 4.5 or greater. This is 5 times the rate of earthquakes in the entire contiguous US (or "lower 48" in Alaska parlance). During this time there have been 11 earthquakes in the U.S. greater than 7.5—all of them have occurred in Alaska.

Based on the recurrence times implied by the 50-year catalog, it is possible to approximate the likelihood of earthquakes of at least a certain size.

There are caveats to this methodology, especially at the largest magnitudes. However, the Alaska seismicity rate is sufficiently high to support this up to magnitudes above 7.

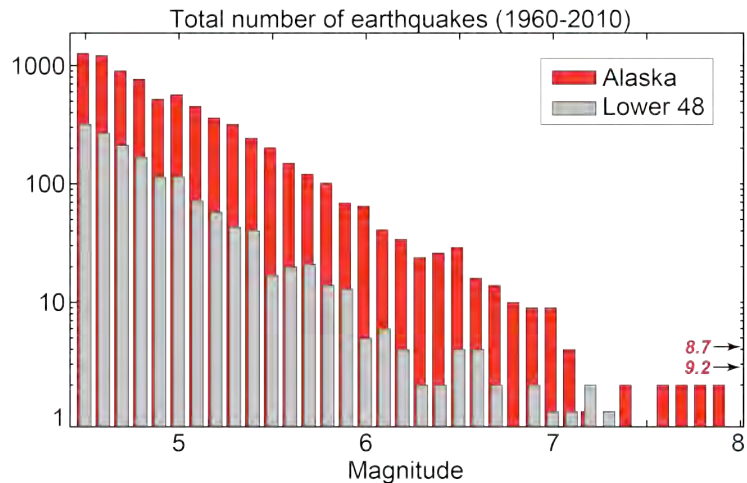


Figure 1. Histogram of earthquakes in Alaska and in the lower 48 states in the past 50 years. Magnitudes for Alaska events¹ are used in order of preference: Mw, Ms, Mb, ml. Magnitudes for the lower 48 are the preferred magnitudes published in the ANSS composite catalog².

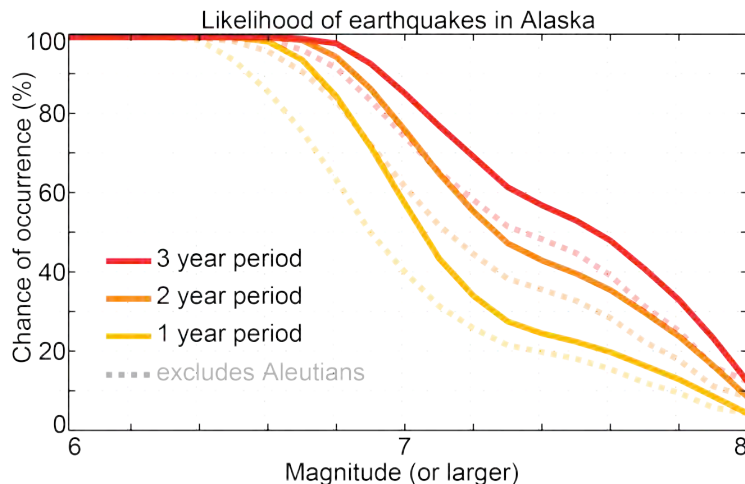


Figure 2. Likelihood of an earthquake occurring with at least a given magnitude. The longer the observation window the greater the chance of an earthquake. The dashed line is the same analysis without including earthquakes in the Aleutian Islands (west of 163°W and south of 57°N)

During a 1-3 year period, an earthquake exceeding 6.5 is a certainty. The likelihood of recording a magnitude 7 or greater is strongly a function of the observation time. There is a 60% chance of a magnitude 7 during a 1-year period, increasing to nearly 90% during a 3-year observation period. While a magnitude 8 earthquake cannot be counted on during a temporary deployment, there is a very real possibility of capturing such an event during the lifetime of a USArray deployment.

Perhaps the most compelling argument for Alaska as a place to understand large earthquakes cannot be observed in figure 2. Magnitude 5 earthquakes occur in Alaska, on average, every 6 days.

Data sources

Alaska earthquake data from the Alaska Earthquake Information Center (www.aeic.alaska.edu)

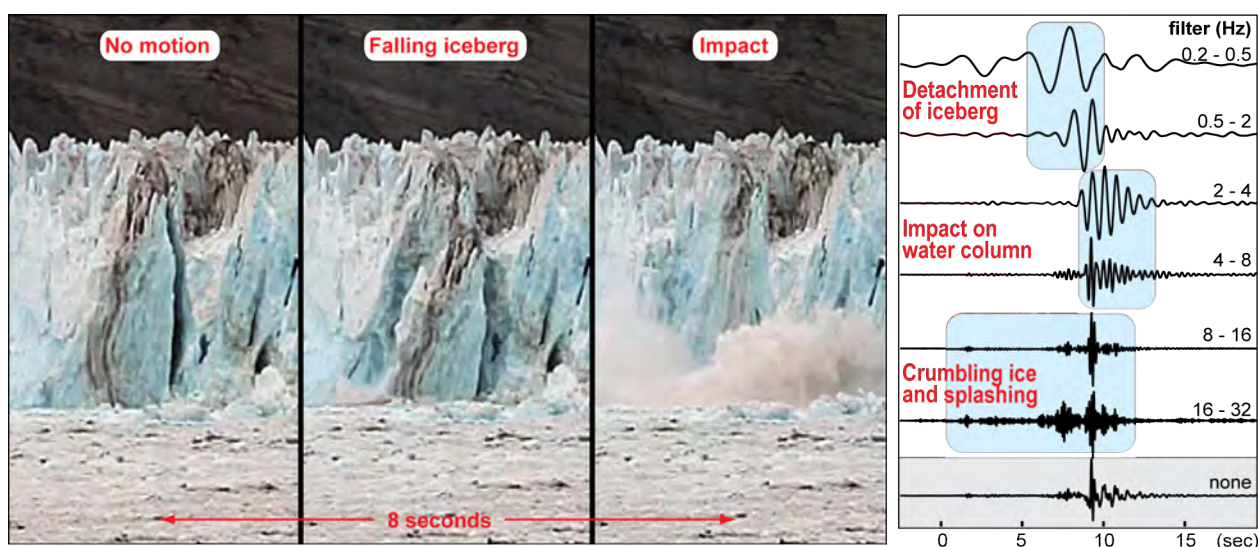
Lower 48 earthquake data drawn from the ANSS composite catalog (<http://www.ncedc.org/cnss/catalog-search.html>)

Toward tracking glacier ice-balance with seismology

Yahtse glacier, Alaska

Michael West, mewest@alaska.edu
Geophysical Institute, Univ. Alaska Fairbanks

Glaciers generate extremely high rates of seismic activity. The largest signals are caused predominantly by iceberg calving at the terminus of tidewater glaciers. A recent surge in glacier seismic studies is providing a new understanding of how calving is manifest seismically. The continuous nature of remote seismic recording, combined with automated detection, proffer this as a technique for long-term 24/7 glacier monitoring. Measuring the ice loss from marine-terminating glaciers remains a key step in determining the flux of freshwater into the oceans. This freshwater is a critical control on sea level, ocean currents, and by extension, climate. Recent experiments in coastal Alaska (e.g. NSF award #0810313) demonstrate the complex but tractable seismic signature of calving (Figure 1). Estimating ice mass remains a challenge, but it is now possible to infer calving activity remotely from continuous seismic records near glaciers.



A calving event at Yahtse glacier, south-central Alaska. Three video frames at left show the detachment and fall of an iceberg from the terminus. A nearby seismic recording (at right) is filtered in several bands to illustrate the multiple overlapping processes that contribute to the signal.

However activity across a regional ice field cannot be extrapolated from a single glacier. Glaciers in close proximity can exhibit wildly different behavior, such as retreating via catastrophic ice loss while adjacent glaciers are advancing. To understand the out flow of an entire ice field, it is necessary to monitoring glaciers on a regional scale.

Earthscope

The broad regional coverage afforded by the Transportable Array (TA) would allow research to expand from a one-glacier-at-a-time technique, to comprehensive calving monitoring across an entire glacier province. The TA, coupled with existing stations, would provide a station density sufficient to track notable calving events at a rate of 10s to 100s per day in Alaska. This real time tracking could even facilitate time-sensitive efforts such as on-call satellite imagery, LIDAR or deployment of on-ice instrumentation, not unlike how the community advances earthquake and volcanic eruption studies through rapid response campaigns.

Searching for precursory events prior to large earthquakes

2002 Denali Fault

Michael West, mewest@alaska.edu
Geophysical Institute, Univ. Alaska Fairbanks

Recent work by Bouchon et al. [Science, 331, 877 (2011)] has shown that the 1999 Izmit, Turkey earthquake was preceded by a remarkable sequence of much smaller earthquakes that demonstrate a tractable relationship to the M_w 7.6 mainshock. The rate of these events accelerated prior to the mainshock and they have a repeating waveform indicating a fixed source and fault mechanism. The multiplet aspect of these earthquakes is an instructive observation but also suggests a mechanism for identifying such sequences even when they elude obvious visual detection.

Spurred by the Izmit sequence, we revisited the 2002 M_w 7.9 Denali Fault Earthquake to establish whether or not similar precursory microearthquakes might have occurred. We use a cross-correlation technique to examine a 22-hour window prior to the earthquake to look for *any* signal in the record that could be identified multiple times. We scan for matching waveforms on all channels (filtered 3-20 Hz) within 100 km of the hypocenter. We also include two hours of the aftershock sequence as it provides a control dataset to validate our approach.

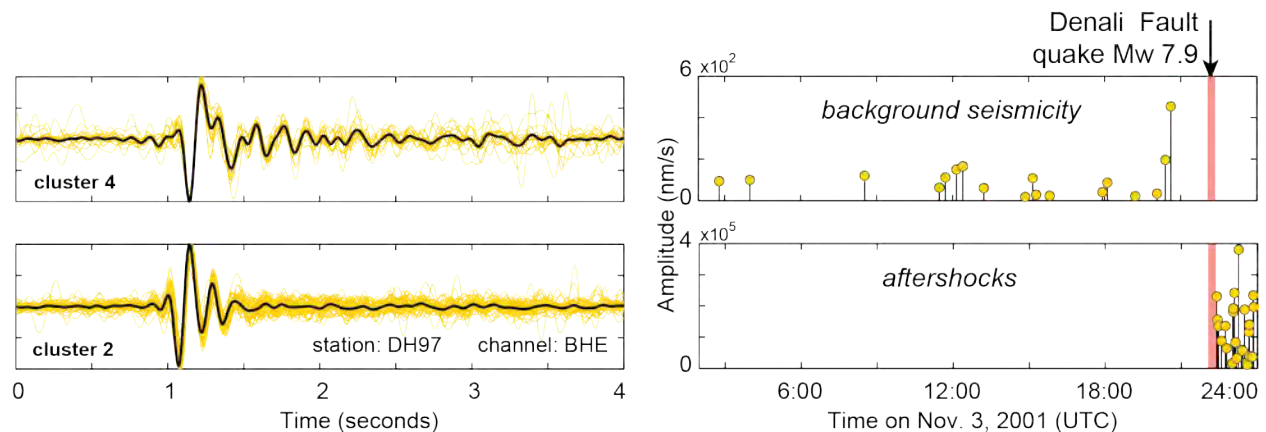


Figure. Repeatedly observed micro-earthquakes and their time-amplitude patterns surrounding the M_w 7.9 Denali Fault Earthquake. The event family on the top is typical of background seismicity. Low amplitude events with this type of on-going time pattern are present on most stations. While they likely reflect minor local tectonics, they show no time association with the Denali Fault Earthquake. Such events are observed on most stations. The waveform on the bottom is one of the countless aftershock event families. Though larger in amplitude and clustered in time, these events do not occur until after the main shock. No comparable families are found prior to the Denali Fault Earthquake.

We find no repeating micro-earthquake activity prior to the Denali Fault earthquake. If such seismicity occurred, it is below the noise floor of existing data. There are several tectonic reasons why this event may not have generated such seismicity. It is also possible that such activity was simply too small to be recorded. While capturing such events requires a degree of serendipity, Alaska's high rate of large earthquakes provides an ideal environment. The Transportable Array would greatly improve the odds of acquiring rare proximal datasets by ensuring a base level of coverage across a vast area. This objective is unlikely to warrant a dedicated Flexible Array deployment. However, the Flexible Array stations are likely to be deployed in higher seismicity regions, making the possibility of a dense near-source nucleation dataset all the more likely.

Recent offshore seismic results and implications for orogenesis and terrane accretion in southern Alaska

Lindsay L. Worthington, Texas A&M University (l.worthington@tamu.edu)

Flat-slab subduction and collision of the Yakutat terrane (YAK) in southern Alaska characterizes the latest iteration of terrane accretion that forms the tectonic assemblage of the Canada-Alaska Cordillera (Figure 1) [Plafker *et al.*, 1994]. Over the last ~10 Myr, the Yakutat slab has subducted ~500 km at a dip of ~6 degrees [Eberhart-Phillips *et al.*, 2006; Gulick *et al.*, 2007], driving orogenesis of the Chugach-St. Elias mountain belt [e.g., Bruhn *et al.*, 2004; Pavlis *et al.*, 2004]. Beyond local uplift, Yakutat-North American convergence has initiated far-field tectonic effects including mantle flow towards Arctic Canada [Mazzotti and Hyndman, 2002] and possible Anatolian-style counterclockwise extrusion of Alaskan crustal blocks westward toward the Bering Sea [Redfield *et al.*, 2007]. Additionally, given the extensive flat-slab segment that the Yakutat terrane forms beneath southern Alaska, many parallels can be drawn to Laramide-style orogeny and deformation, lending insight into the evolution of the western continental United States. Recent offshore seismic results lend insight into major questions regarding velocity structure, thickness and composition of the Yakutat terrane itself that have previously gone unanswered.

A two-dimensional seismic velocity model [Worthington *et al.*, in review] of the Yakutat terrane based on joint inversion of coincident marine seismic reflection and refraction data collected as part of the St. Elias Erosion and Tectonics Project (STEET) shows that the offshore Yakutat terrane is wedge-shaped. Yakutat crust tapers in the direction of subduction from ~30 km thick east of the DRZ to ~17 km thick near Bering Glacier. After the initial taper observed offshore, subducted Yakutat thickness remains relatively constant, resulting in flat-slab subduction and anomalously thick low-velocity zones beneath Prince William Sound and as far inboard as the Alaska Range. The thickest Yakutat crust enters the St. Elias orogen north of Malaspina Glacier, where the orogen displays its highest relief and highest long-term exhumation rates. Uplift patterns and present-day St. Elias topography are likely controlled by the interplay of lateral variations in the Yakutat terrane “door stop” geometry at depth and the restraining-bend geometry of surface faults. The model also includes a low-velocity zone at the eastern end of the profile with seismic velocities and possible onshore equivalents consistent with a remnant accretionary prism. The internal structure of the Yakutat crust suggests that the terrane formed as an oceanic plateau that accreted mélange sediments during an episode of terrane collision that predates the present convergence with North America in the St. Elias region.

Given proposed limits on subductibility of thickened oceanic lithosphere, we suggest that Yakutat terrane subduction in southern Alaska will eventually cease. It is likely that the Transition Fault will become the major transform plate boundary between North America and the Pacific Plate in the northern Gulf of Alaska and some portion of the subducted Yakutat terrane will underplate North America while the unsubducted Yakutat terrane material will become part of the North American continent. This interpretation may provide insight into the mechanisms for Laramide uplift in the western US and into the ongoing process of terrane accretion in southern Alaska.

References

- Bruhn, R. L., T. L. Pavlis, G. Plafker, and L. Serpa (2004), Deformation during terrane accretion in the St. Elias orogen, Alaska, *Geological Society of America Bulletin*, 116(7-8), 771-787.
- Eberhart-Phillips, D., D. H. Christensen, T. M. Brocher, R. Hansen, N. A. Ruppert, P. J. Haeussler, and G. A. Abers (2006), Imaging the transition from Aleutian Subduction to Yakutat collision in central Alaska, with local earthquakes and active source data, *Journal of Geophysical Research*, 111(B11303), 1-31.
- Gulick, S. P. S., L. A. Lowe, T. L. Pavlis, J. V. Gardner, and L. A. Mayer (2007), Geophysical insights into the Transition Fault debate: Propagating strike-slip in response to stalling subduction in the Gulf of Alaska, *Geology*, 35(8), 763-766.
- Mazzotti, S., and R. D. Hyndman (2002), Yakutat collision and strain transfer across the northern Canadian Cordillera, *Geology*, 30(6), 495-498.
- Pavlis, T. L., C. Picornell, L. Serpa, R. L. Bruhn, and G. Plafker (2004), Tectonic processes during oblique collision: Insights from the St. Elias orogen, northern North American Cordillera, *Tectonics*, 23(TC3001).
- Plafker, G., J. C. Moore, and G. R. Winkler (1994), Geology of the southern Alaska margin, in *The Geology of Alaska*, edited, pp. 389-449, The Geological Society of America, Denver.
- Redfield, T. F., D. W. Scholl, P. G. Fitzgerald, and M. E. Beck, Jr. (2007), Escape tectonics and the extrusion of Alaska; past, present, and future, in *Geology [Boulder]*, edited, pp. 1039-1042, Geological Society of America (GSA) : Boulder, CO, United States, United States.